Received: 2 January 2019 | Revised: 25 March 2019 | Accepted: 7 May 2019
DOI: 10.1002/tal.1630

RESEARCH ARTICLE

WILEY

Shaking table test and numerical analysis of an asymmetrical twin-tower super high-rise building connected with long-span steel truss

Wei Guo[1,2,3] | Zhipeng Zhai[1,2,3] | Hanfeng Wang[1,2] | Qiongxiang Liu[4] | Kai Xu[4] | Zhiwu Yu[1,2,3]

[1] School of Civil Engineering, Central South University, Changsha, China
[2] National Engineering Laboratory for High Speed Railway Construction, Changsha, China
[3] Engineering Technology Research Center for Prefabricated Construction Industrialization of Hunan Province, Changsha, China
[4] Shenzhen General Institute of Architectural Design and Research Co., Ltd., Shenzhen, China

Correspondence
Zhipeng Zhai, School of Civil Engineering, Central South University, Changsha 410075, China.
Email: zhaizhipeng@csu.edu.cn

Funding information
Project of Yuying Plan in Central South University, Grant/Award Number: 502034002; Foundation for Key Youth Scholars in Hunan Province, Grant/Award Number: 150220077; National Natural Science Foundation of China, Grant/Award Number: 51878674; Fundamental Research Funds for the Central Universities of Central South University, Grant/Award Number: 502221804

Summary
The asymmetrical high-rise building investigated in this paper is composed of a 299.1-m-high tower and a 235.2-m-high tower, which are diagonally and rigidly connected by two steel truss systems with the maximum span of 65.43 m. Given the great structural irregularities and complexities, the structural seismic performance is necessary to be investigated. A shaking table test of a 1/45 scaled model is conducted in this study, by which the structural damage pattern and dynamic responses are analyzed. The results show that the connecting trusses and rigid connection joints behave well during strong seismic excitations. The damages concentrate on the connecting floors, and the whole structural damage is slight. Most of the lateral resistance components remain elastic. The structure presents high seismic resistance against strong ground motions. Subsequently, a three-dimensional finite element model of prototype structure is established and validated by the experimental results. The analyses indicate that performance of the connecting trusses is capable of coordinating translational and torsional deformation of the two towers and making them resist lateral seismic force together even subjected to maximum considered earthquakes. And this performance is still reliable although the high torsional modes are triggered.

KEYWORDS
asymmetrical connected structure, long-span steel truss, numerical analysis, seismic performance, shaking table test, supertall towers

1 | INTRODUCTION

With the advancements of high-performance materials and construction techniques, the past decades have witnessed a boom of super high-rise buildings throughout the world. Many complex skyscrapers, such as Shanghai World Financial Center Tower, Taipei 101, and Shanghai Tower, have been built.[1–3] In recent years, to meet the requirement of transportation convenience and architectural esthetics, multitower connected structure has been gradually employed in practical engineering, such as Petronas Twin Towers (452 m high), CCTV Main Building (234 m high), and the Island Tower Sky Club (145.3 m high).[4,5] Corridors are often used to connect the towers, and the connection joint between corridors and towers can be classified as two types: rigid joint and flexible joint. No matter which connection type is adopted, seismic performance is the critical issue due to the irregularity and complexity of connected structure.

The flexible connection joint allows the corridor to move relatively to the primary structure but does not coordinate the displacement between the towers. It should be noted that large slip displacement of the connection may cause collision with the primary structure and induce collapse of the connection. Therefore, damping devices are usually used to reduce the seismic response and control the slip displacement. Wu[4] performed finite element analysis of a four-tower connected structure in which the connection between the towers was designed as flexible link by using friction pendulum bearings and viscous dampers. The optimal design of bearings and dampers were conducted. The results showed that the energy dissipation devices have well effect on seismic reduction. Shaking table test of the four-tower connected structure is then conducted by Lu.[6] The results showed that the protective system with viscous dampers reduced the seismic response of the sky corridor. The sky corridor keeps in elastic state under strong earthquakes. Other researches[5,7,8] have also verified the effectiveness of using viscoelastic dampers between building and sky corridor connections to reduce seismic response.

Connection joint between the corridor and the towers also can adopt rigid design, especially for long-span connection. The rigid connection joint by which the corridor is generally connected to core tube or shear wall of the primary structure can coordinate the displacement between the towers. And the connection is protected by the stiffness of towers. Zhou[9] performed shaking table test for a multitower hybrid structure. The results showed that although the steel members buckled under earthquakes, the rigid joints between the connecting steel truss and the core walls worked well. Lu[10] conducted shaking table test on a complex high-rise building with two towers of different heights connected by trusses. The results revealed that stiffness of the connecting trusses is able to coordinate the two towers to resist lateral forces jointly. To fully investigate seismic performance of the two towers, numerical analysis was performed by using three software programs.[11] And seismic safety of the two towers with rigid connection was validated. Similarly, Wu[12] utilized the finite element method to assess seismic performance of an asymmetrical twin-tower rigid connected structure. The effectiveness of rigid connection joint used for the asymmetrical connected structure is proved and reasonable energy dissipation mechanism of the connected structure is achieved.

Due to lateral stiffness mutation and dynamic interaction of the towers in rigid connected structure, the stress state of the connection joints will be more complicated under seismic excitations, and the internal force between connection and towers will be larger.[4,6] In other word, rigid connected structure may be more vulnerable to subject high intensity earthquakes. Previous studies also illustrated that large vertical acceleration under strong ground motions will cause large deformation and stress of long-span connecting truss.[9,13] As the long-span connecting truss may be sensitive to the vertical excitations, the soil-structure interaction is also a critical factor that significantly affects the seismic performance of connected structure.[14–17] Moreover, some surveys of post earthquake showed that the larger the connection span is or the stronger the structural asymmetry is, the more serious the structural damage is.[13] Therefore, it is necessary to evaluate the seismic performance of asymmetrical rigid connected structure with long-span connection.

Shaking table test is an effective approach to investigate the seismic behavior and failure mechanism of structures.[18–21] It is widely used for the irregular structures, such as complex supertall buildings and multitower connected structures,[6,18,19,22] which are not currently included in the design codes. The complex structure investigated in this study is an asymmetrical twin-tower super high-rise building, which is rigidly connected by long-span steel truss. The two single towers without truss connections differ greatly in fundamental period, which is a difference of 1.7 s as a result of large different structural height. Furthermore, they are connected by two diagonal steel truss systems located at low zone (fifth to eighth floor) and high zone (33rd–36th floor), respectively. These indicate that the torsional effect of the structure will be significant. Thus, seismic safety of the overall structure, performance of rigid connection joints, and connecting truss performance of coordinating two towers' deformation are the critical issues needed to be assessed. In this study, a 1/45 scaled model of the twin-tower super high-rise building is constructed and tested on the shaking table. The behavior of test specimen under service level earthquake (SLE), design-based earthquake (DBE), and maximum considered earthquake (MCE) is considered in the test. And the three-directional excitation of ground motions is also taken into account. By the test, the dynamic responses and damage pattern of the test specimen are analyzed. Finally, a detailed numerical model of the prototype structure is presented based on ETABS. Also, nonlinear time history analyses are implemented, and the numerical results are compared with the experiment to obtain a better understanding for the structural behavior.

2 | DESCRIPTION OF THE BUILDING STRUCTURE

2.1 | The main building

The prototype building, Shenzhen Bay Innovation and Technology Centre (SBITC), consists of two super tall towers with different height and two steel truss systems, is shown in Figure 1. It is built in Shenzhen, China, and is designed in accordance with the Chinese Code for Seismic Design of Buildings (GB50011-2010).[23] The two towers adopt frame-tube structure system composed of steel tube-reinforced concrete (RC) column, RC core wall, and horizontal brace, which are combined to resist vertical and lateral loads. The structural heights of Tower A and Tower B are 299.1 and 235.2 m, respectively. In the two towers, the first and fourth floor heights are both 6 m, second floor is 5.1 m, third floor is 4.5 m, refuge floors are 5.1 m, and other standard floors are 4.2 m. Elevation view of SBITC is plotted in Figure 2. Plane sizes of the two towers are both 45 m × 45 m. Plane size of core tube of Tower A is 27.15 m × 21.30 m below the 40th floor and reduces as 22.15 m × 19.70 m above the 40th floor. For Tower B, it is 26.00 m × 20.40 m below the 40th floor and reduces as 21.70 m × 19.70 m above the 40th floor. Steel tube-RC column is adopted for frame column below the 43rd floor of Tower A and 38th floor of Tower B. The other frame columns use RC column. The plane layout of SBITC

FIGURE 1 Architectural visualization of Shenzhen Bay Innovation and Technology Centre

is shown in Figure 3. The dimension of main structural members of the two towers is listed in Table 1. The main materials employed for SBITC include C35 and C60 concrete with the nominal compressive strength of 35 and 60 MPa, HRB400 reinforcement with nominal yield strength of 400 MPa, and Q345 steel with nominal yield strength of 345 MPa.

2.2 | The connecting trusses

Two diagonal steel truss systems are designed based on Chinese code[23] to rigidly connect the two towers. They are extended to core tube or shear wall of the primary structure and locate at low zone (fifth to eighth floor) and high zone (33rd–36th floor), respectively. The maximum spans for the two steel truss systems are 57.8 and 65.43 m, respectively. To prevent the floor slab cracking during the normal service period, horizontal braces are set in the connecting floors. Details of the connecting steel trusses are depicted in Figure 4, and the designing dimension of main structural members in the connecting steel trusses is listed in Table 2.

According to the Chinese Code for Seismic Design of Buildings (GB50011-2010)[23] and the *Technical Specification for Concrete Structures of Tall Building* (JGJ3-2011),[24] the main structural irregularities of the twin-tower connected structure can be summarized as follows:

1. The structural heights of the two towers, 299.1 and 235.2 m, beyond the limit of JGJ3-2011[24] in which the maximum structural height is prescribed as 190 m for hybrid structure in regions with seven degrees of seismic fortification intensity.
2. There are large openings in the second and third floor, which have a floor area of over 30% and beyond the limit specified in JGJ3-2011.[24] Meanwhile, it results in the floor slab discontinuity.
3. In elevation, the two towers with great difference in structural height are diagonally connected by two steel truss systems. Furthermore, both the towers and the steel trusses are asymmetrical, and plane size of the core tube is reduced above 40th floor. All these result in the sudden change of the lateral stiffness of the towers along the structural height and will make the structural seismic behavior more complicated.
4. Span of connecting steel truss is generally assumed to be 12–60 m in practical engineering. However, the maximum truss span of the structure in this paper reaches 65.43 m. And this truss is diagonally and rigidly connected with the main structure at the high zone. Even small relative torsion of the two towers will induce large internal force in the trusses.

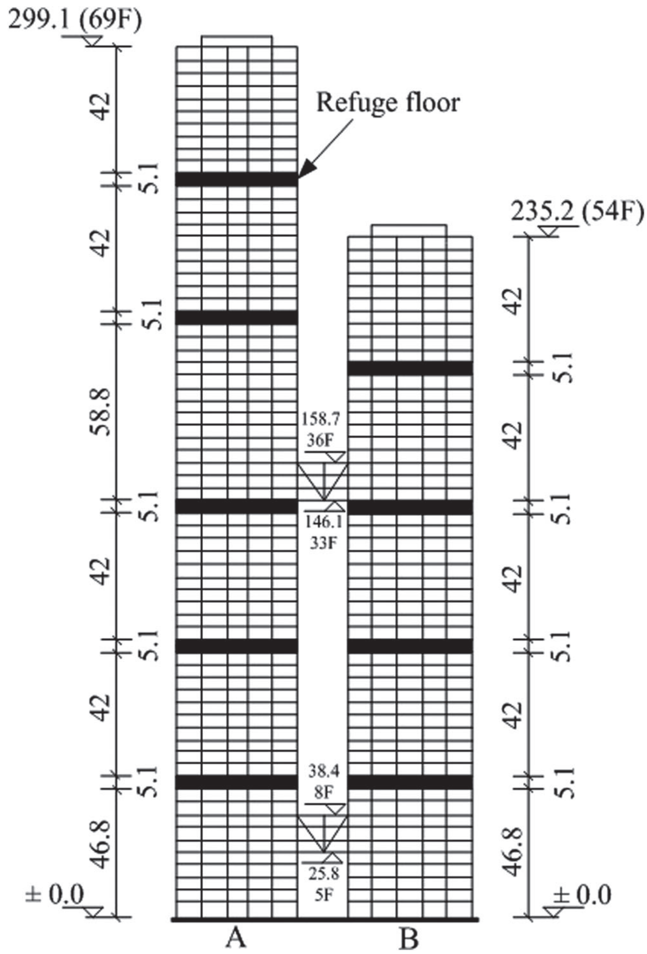

FIGURE 2 Elevation of Shenzhen Bay Innovation and Technology Centre (m)

3 | SHAKING TABLE TEST OF THE MODEL STRUCTURE

The shaking table test is conducted by the shaking table array system in Central South University, China. The system is composed of four shaking tables and can produce six degrees of freedom. Each table is 4 m long and 4 m wide. The maximum payload of each table is 300 kN, and the corresponding maximum acceleration for horizontal and vertical directions is 0.8 and 1.6 g, respectively. The maximum velocity is 1,000 mm/s, and the effective frequency ranges from 0.1 to 50 Hz. These tables can be used independently and can also make up an array system with various adjustable spacing. In this paper, one shaking tale is used for the structural model test.

3.1 | Model design and construction

To investigate the seismic performance of super tall building, small scaled model test is frequently used. It is impossible to use prototype material for constructing the model structure. And the model material should behave similarly to the prototype material.[25] In this model, fine aggregate concrete with fine iron wire is utilized to construct RC components of the prototype structure. The steel tube of the frame columns in prototype structure is simulated by stainless steel, the connecting steel truss is simulated by copper plate, and the other steel members are simulated by section steel. The compressive strength and elastic modulus of the fine aggregate material are listed in Table 3.

To make sure that the scale model behaves in a similar manner to the prototype, the model should be designed in accordance with dynamic similitude theory. Harris[26] has systematically introduced the similitude theory and the applications of structural model testing. The dynamic similarity principle for shaking table test can be expressed as

$$S_E/S_\rho S_a S_l = 1, \tag{1}$$

where S_E, S_ρ, S_l, and S_a are scaling factors of elastic modulus, mass density, dimension, and acceleration, respectively. Although three of the four factors are chosen, the similar relationship then will be determined. Considering the capacity and size of the shaking table, S_l is set to be 1/45.

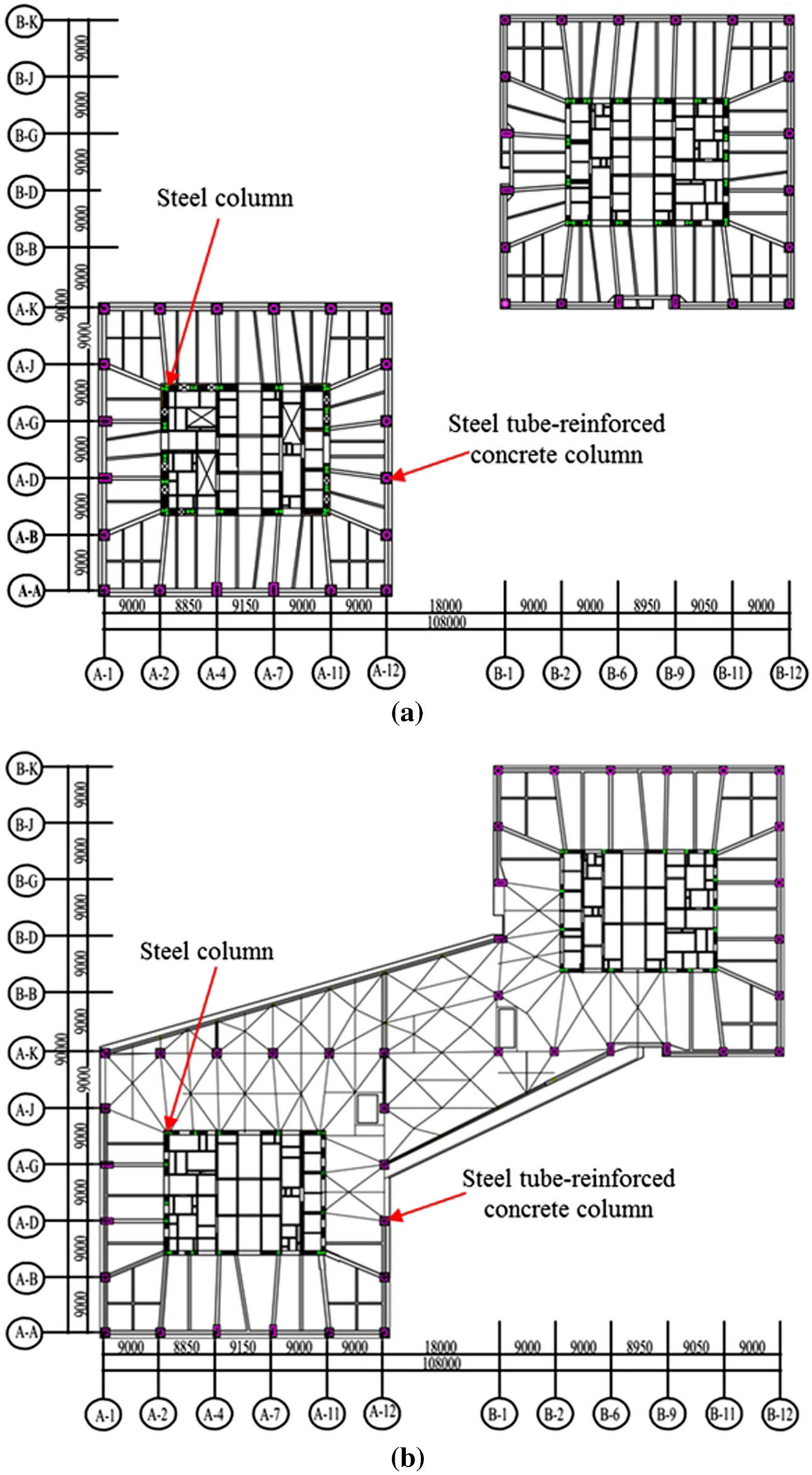

FIGURE 3 Plan layout of Shenzhen Bay Innovation and Technology Centre (mm). (a) Standard floor plan. (b) Typical connecting floor plan

According to the material test results, the overall scaling factor of the elastic modulus is adopted as 0.3. S_a is chosen to be 3 in this test, and additional mass blocks are evenly distributed on the model to compensate for the difference in vertical load. The total mass of the model is about 19,120 kg, containing mass blocks 15,040 kg. The test structure is casted on a rigid RC foundation with dimensions of 3.2 m long × 2.7 m wide × 0.3 m high and the total mass of about 6,480 kg. The foundation is fixed on the shaking table by high strength bolts, and sliding is not allowed during the test. The main parameter's similarity scaling factors of the specimen are shown in Table 4.

The members of test model are designed based on the similarity principle of structural members. For the RC structural members, bending resistance and shear resistance equivalent principle are used to control bearing capacity of cross section and oblique section, respectively. The model reinforcement can be calculated using Equations (2) and (3). For steel members (not containing steel truss members), equivalent principle of

TABLE 1 Dimension of the main structure members (unit: mm)

	Tower A					Tower B			
	Column		Beam	Shear wall		Column		Beam	Shear wall
Floor	*l* × *b*	*d* × *t*	*b* × *h*	*t*	Floor	*l* × *b*	*d* × *t*	*b* × *h*	*t*
1–4	1,800 × 1,800	1,400 × 40	900 × 600	1,300	1–10	1,500 × 1,500	1,100 × 30	900 × 500	1,000/900
5–10	1,700 × 1,700	1,300 × 40	900 × 600	1,200	11–20	1,400 × 1,400	1,000 × 25	900 × 500	900/700
11–19	1,600 × 1,600	1,200 × 30	900 × 600	1,100	21–29	1,300 × 1,300	900 × 25	900 × 500	700/600
20–28	1,500 × 1,500	1,100 × 30	900 × 600	900	30–37	1,200 × 1,200	800 × 25	900 × 500	600
29–42	1,400 × 1,400	1,000 × 25	900 × 600	800/700/600	38–39	1,100 × 1,100		900 × 500	600
43–54	1,400 × 1,400		900 × 600	600	40–roof	1,000 × 1,000		900 × 500	600/400
55–59	1,200 × 1,200		900 × 600	600/400					
60–roof	1,000 × 1,000		900 × 600	600/400					

Note. *l*, length; *b*, width; *t*, thickness; *h*, height; *d*, external diameter of circular steel tube.

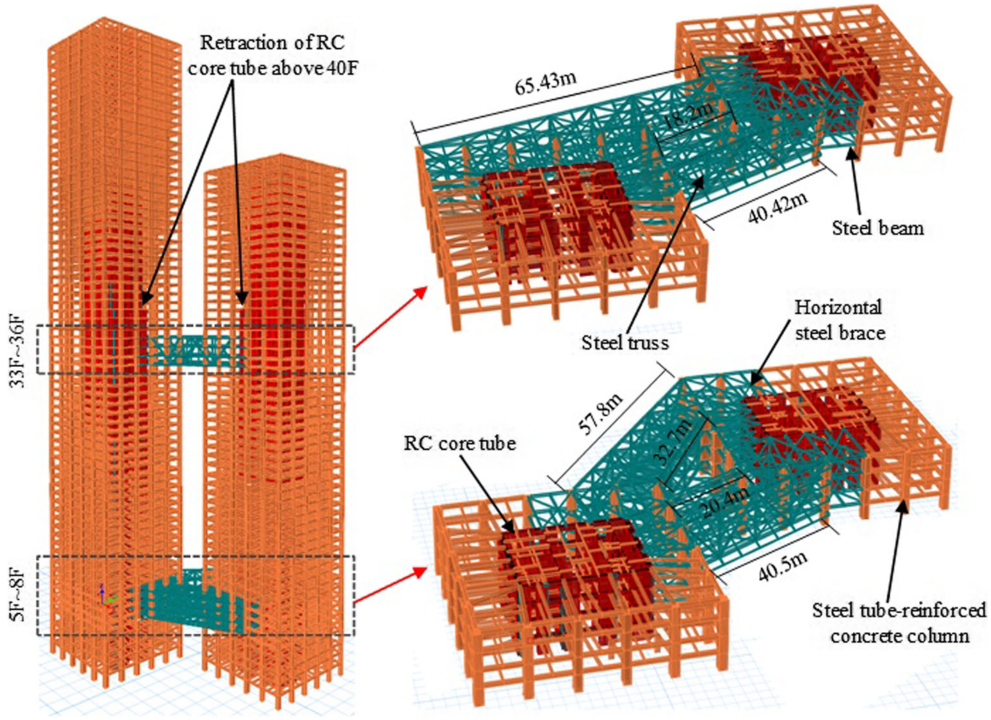

FIGURE 4 Connecting steel trusses of Shenzhen Bay Innovation and Technology Centre. RC, reinforced concrete

TABLE 2 Dimension of the main members in connecting steel trusses (unit: mm)

Members	Section in 5F–8F	Section in 33F–36F
Truss chord member	H800 × 500 × 20 × 35; H900 × 500 × 20 × 45 H1000 × 500 × 20 × 40	H800 × 500 × 20 × 35; H900 × 500 × 20 × 45 H1000 × 500 × 20 × 40
Truss vertical member	□500 × 400 × 30 × 30	□500 × 400 × 30 × 30; □500 × 500 × 30 × 30
Truss web member	□500 × 400 × 30 × 30 □500 × 500 × 30 × 30	□500 × 400 × 30 × 30; □500 × 500 × 30 × 30 □600 × 500 × 40 × 30
Horizontal brace in floor slab	H400 × 200 × 8 × 13; H400 × 250 × 10 × 20 H500 × 250 × 12 × 20; H500 × 300 × 25 × 20	H400 × 200 × 8 × 13; H400 × 250 × 10 × 20 H500 × 250 × 12 × 20; H500 × 300 × 25 × 20 H500 × 350 × 25 × 35

Note. H, H section steel tube; □, square steel tube.

TABLE 3 Compressive strength and elastic modulus of fine aggregate concrete

Series	Compressive strength (MPa)	Elastic modulus (10^4MPa)	Elastic modulus of prototype materials (10^4MPa)	Ratio of elastic modulus
1	15.21	0.95	3.60	0.26
2	11.18	1.37	3.60	0.38
3	12.14	1.49	3.60	0.41
3	6.92	0.73	3.15	0.23
4	5.45	0.60	3.15	0.19
5	5.08	0.87	3.15	0.28

TABLE 4 Similarity scaling factors of the test model

Parameter	Relation	Scaling factors	Parameter	Relation	Scaling factors
Length l	S_l	1/45	Uniform load q	$S_q = S_\sigma S_l$	6.67×10^{-3}
Stress σ	$S_\sigma = S_E$	0.3	Area load p	$S_p = S_\sigma$	0.3
Elastic modulus E	S_E	0.3	Moment M	$S_M = S_\sigma S_l^3$	3.29×10^{-6}
Strain ε	S_ε	1	Period T	$S_T = (S_l/S_a)^{0.5}$	8.61×10^{-2}
Density ρ	$S_\rho = S_E/(S_a S_l)$	4.5	Frequency f	$S_f = (S_a/S_l)^{0.5}$	11.6
Mass m	$S_m = S_\rho S_l^3$	4.94×10^{-5}	Acceleration a	S_a	3
Concentrated force F	$S_F = S_\sigma S_l^2$	1.48×10^{-4}	Gravitational acceleration g	S_g	1

bending and axial stiffness is employed to design the steel section, which is expressed as Equations (4) and (5). The steel truss members are designed by the axial force equivalent principle given as Equation (6).

$$A_s^m = A_s^p \frac{S_M}{S_l S_{f_y}} = \frac{S_\sigma}{S_{f_y}} S_l^2 A_s^p, \tag{2}$$

$$A_{sv}^m = A_{sv}^p \frac{S_V}{S_{f_{yv}} S_l} S_s = \frac{S_\sigma}{S_{f_{yv}}} S_l S_s A_{sv}^p, \tag{3}$$

$$\frac{E^m I^m}{E^p I^p} = S_E S_l^4, \tag{4}$$

$$\frac{E^m A^m}{E^p A^p} = S_E S_l^2, \tag{5}$$

$$A_{tr}^m = S_N \frac{A_{tr}^p}{S_{f_{tr}}} = \frac{S_\sigma}{S_{f_{tr}}} S_l^2 A_{tr}^p, \tag{6}$$

where superscript m and p refers to the model structure and the prototype structure, respectively. A_s is a cross-sectional area of the longitudinal reinforcement in tension; A_{sv} is a cross-sectional area of stirrups with different legs; S_σ, S_{fy}, S_{fyv}, and S_s are the scaling factors of stress, tensile strength of reinforcement, tensile strength of stirrups, and spacing of stirrups, respectively. E is elastic modulus of steel materials, I is the inertia moment, and A is the cross-sectional area of steel members. A_{tr} is cross-sectional area of truss members, S_N is the scaling factor of axial force, and S_{ftr} is the scaling factor of tensile strength between steel and copper plate.

During the test model construction, secondary beams were simplified to make the construction easy. Considering that the main function of secondary beams is only to resist the vertical loads transmitted through slab and it provides little contribution to lateral stiffness of the overall structure, the stiffness of secondary beams was transformed into slab based on the stiffness equivalence.[18] Moreover, the effect of stiffener plate in truss members was ignored due to the results of the axial compressive and bending test of truss members indicated that failure state of truss members is obviously a global buckling instead of local bucking (Figure 5), and it is difficult to construct such small plates in the laboratory as a result of small model scale and small thickness of the stiffener plates. The construction of test model structure is shown in Figure 6.

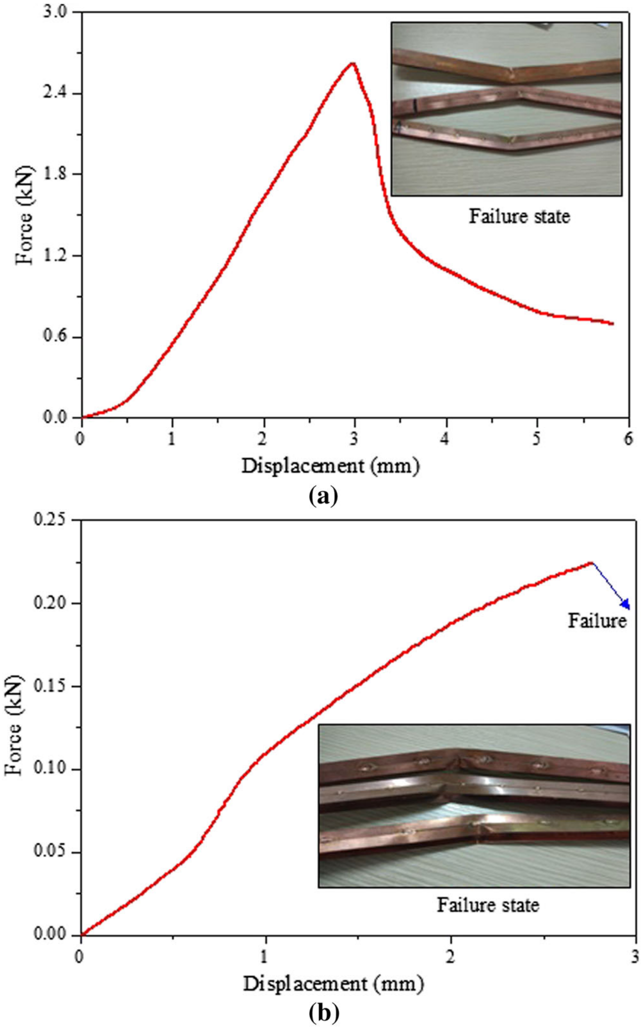

FIGURE 5 Failure state of truss member under static testing. (a) Axial compressive test. (b) Bending test

3.2 | Instruments and sensors

The test setup was equipped with accelerometers, laser displacement sensors, and strain gages for measurement with sampling frequency of 1,000 Hz. Figure 7 shows the locations of the accelerometers and displacement sensors. Forty-eight accelerometers were placed, including three on the rigid foundation, 23 on the Tower A, 20 on the Tower B, and two on the connecting truss. Few measurement points are installed with vertical accelerometer to capture the structural vertical response, such as Z-directional accelerometers on the connecting trusses. Thirty laser displacement sensors were placed, including four on the foundation, 14 on the Tower A, and 12 on the Tower B. In addition, 50 strain gages were attached on the important elements of the connected structure, such as truss members and connecting joints between column and truss, to investigate the inelastic behavior of the towers and connecting trusses.

3.3 | Loading history

Three ground motions, including two earthquake records (E1 and E2) and an artificial seismic motion, are selected according to the Chinese code.[23] The comparison of response spectrum between the selected ground motions and the design spectrum under seismic intensity level of SLE is shown in Figure 8. In this figure, E1-Y represents Y-directional component of ground motion E1, and the other terms are similar. Before the ground motions are input, duration and amplitude of the motions would be scaled according to the similarity scaling factors.

The peak ground acceleration (PGA) of the input seismic excitations is increased from 0.105 to 0.3, 0.66, and 0.875 g. The PGA of 0.105, 0.3, and 0.66 g represents the seismic intensity level of SLE, DBE, and MCE, respectively. For SLE and DBE shaking level, the specimen was first loaded in X and Y-direction, separately. Then, it was loaded in three directions, and the input PGA ratio of principal direction to other directions is 1:0.85:0.65. For MCE shaking level, the specimen was first loaded in X and Y-direction, separately. Then, it was loaded in bidirection and the input

FIGURE 6 Construction of the test model structure. (a) Structural member manufacture. (b) Connecting truss of fifth to eighth floor. (c) Connecting truss of 33rd–36th floor. (d) The test model

PGA ratio of X to Y-direction is 1:0.85. For shaking level with PGA of 0.875 g, the specimen was only loaded in X and Y-direction, separately. To identify the dynamic characteristics and overall damage state of the test specimen, white noise with small magnitude is loaded after each seismic level in bidirection. During the test, 39 seismic loading cases are performed for the specimen in total, which are shown in Table 5.

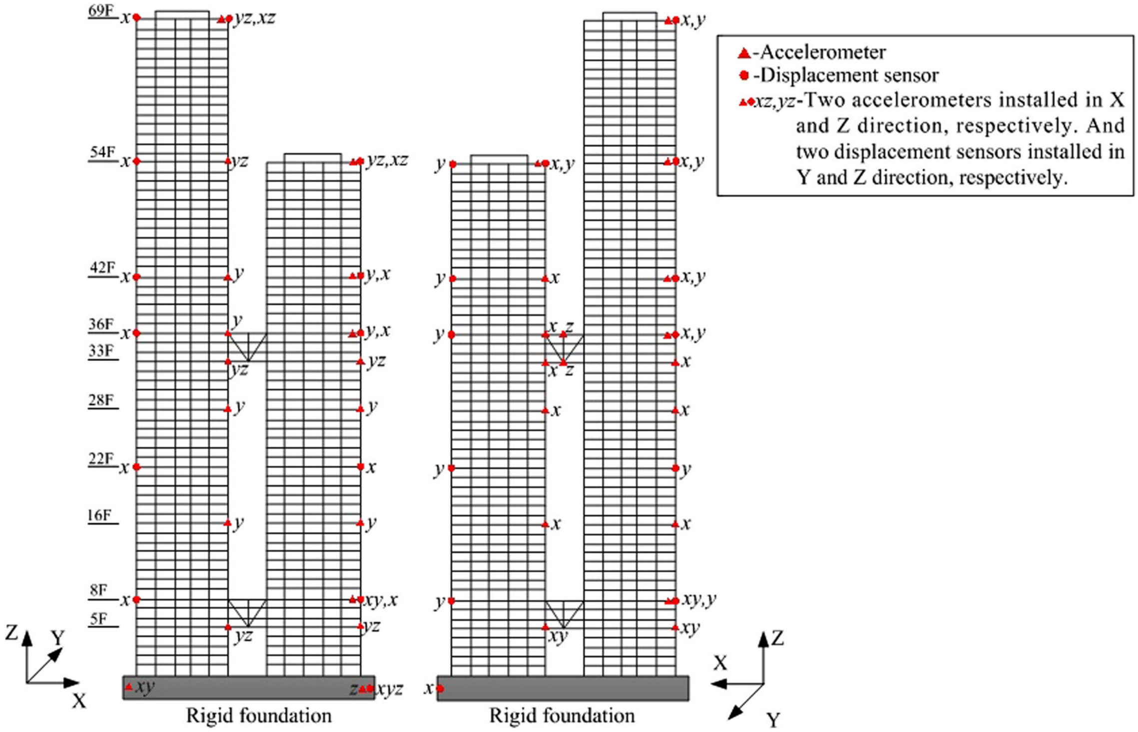

FIGURE 7 Arrangement of accelerometers and displacement sensors

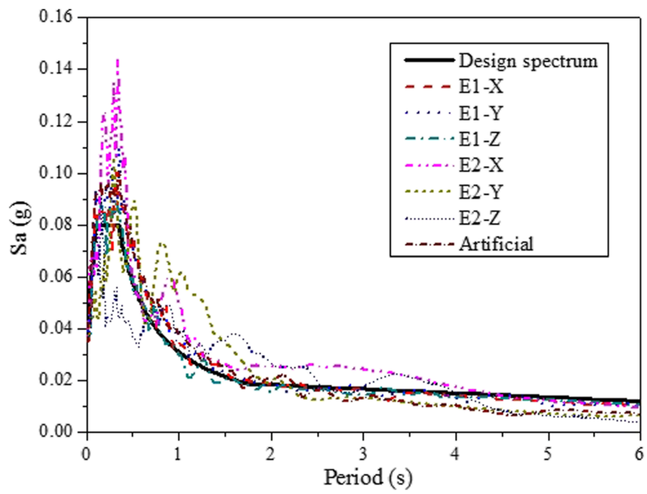

FIGURE 8 Acceleration response spectrum of seismic excitations scaled to service level earthquake

4 | EXPERIMENTAL RESULT AND ANALYSIS

4.1 | Damage observations

Damages of the two towers and connecting steel trusses observed during the test are described as follows. For SLE level excitations with PGA = 0.105 g, no visible damage is observed. Under DBE level excitations with PGA = 0.3 g, fine crack and local concrete spalling occurred at the corner column of the eighth floor of Tower A, as depicted in Figure 9a. Meanwhile, concrete spalling of corner columns at the sixth and seventh floor of Tower A is also observed, as plotted in Figure 9b. For the MCE level input with PGA = 0.66 g, corner columns of Tower B at sixth and eighth floor spalled slightly, which are shown in Figure 9c,d, respectively. Under the excitations of seismic level with PGA = 0.875 g, local slight buckling occurred in several truss members, such as truss chord member at eighth floor and truss web member at 35th floor, as displayed in Figure 10.

TABLE 5 Seismic loading cases

Case	Earthquake	Input PGA (g) X	Y	Z	Case	Earthquake	Input PGA (g) X	Y	Z
WN	White noise	0.05	0.05		21	Artificial	0.3		
1	E1	0.105			22			0.3	
2			0.105		23		0.3	0.255	0.195
3		0.105	0.089	0.068	24		0.255	0.3	0.195
4		0.089	0.105	0.068	WN	White noise	0.05	0.05	
5	E2	0.105			25	E1	0.66		
6			0.105		26			0.66	
7		0.105	0.089	0.068	27		0.66	0.561	
8		0.089	0.105	0.068	28	E2	0.66		
9	Artificial	0.105			29			0.66	
10			0.105		30		0.66	0.561	
11		0.105	0.089	0.068	31	Artificial	0.66		
12		0.089	0.105	0.068	32			0.66	
WN	White noise	0.05	0.05		33		0.66	0.561	
13	E1	0.3			WN	White noise	0.05	0.05	
14			0.3		34	E1	0.875		
15		0.3	0.255	0.195	35			0.875	
16		0.255	0.3	0.195	36	E2	0.875		
17	E2	0.3			37			0.875	
18			0.3		38	Artificial	0.875		
19		0.3	0.255	0.195	39			0.875	
20		0.255	0.3	0.195	WN	White noise	0.05	0.05	

Abbreviation: PGA, peak ground acceleration.

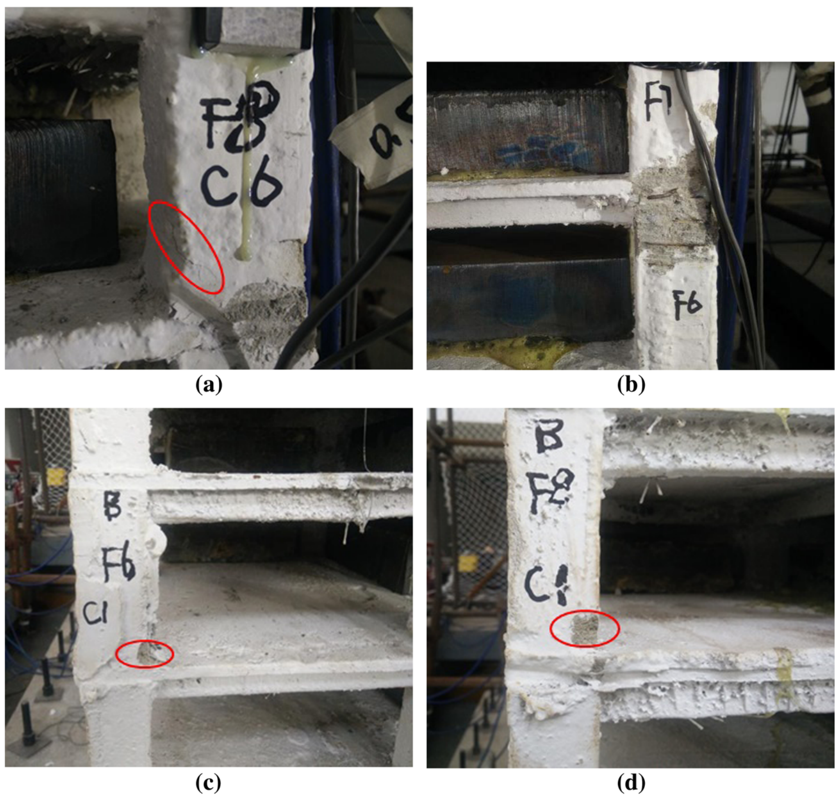

FIGURE 9 Damage of the towers. (a) Crack and concrete spalling of corner column at eighth floor of Tower A. (b) Concrete spalling of corner column at sixth and seventh floor of Tower A. (c) Concrete spalling of corner column at sixth floor of Tower B. (d) Concrete spalling of corner column at eighth floor of Tower B

According to the test observations, most serious damage of the test model is the local concrete spalling at few frame columns. Damage of the two towers concentrates on the corner columns, because stress on corner columns is larger than the others as a result of shear leg effect in frame-tube structure. Damage of Tower A occurred prior to Tower B due to larger structural height. All damage of the towers located at the sixth to

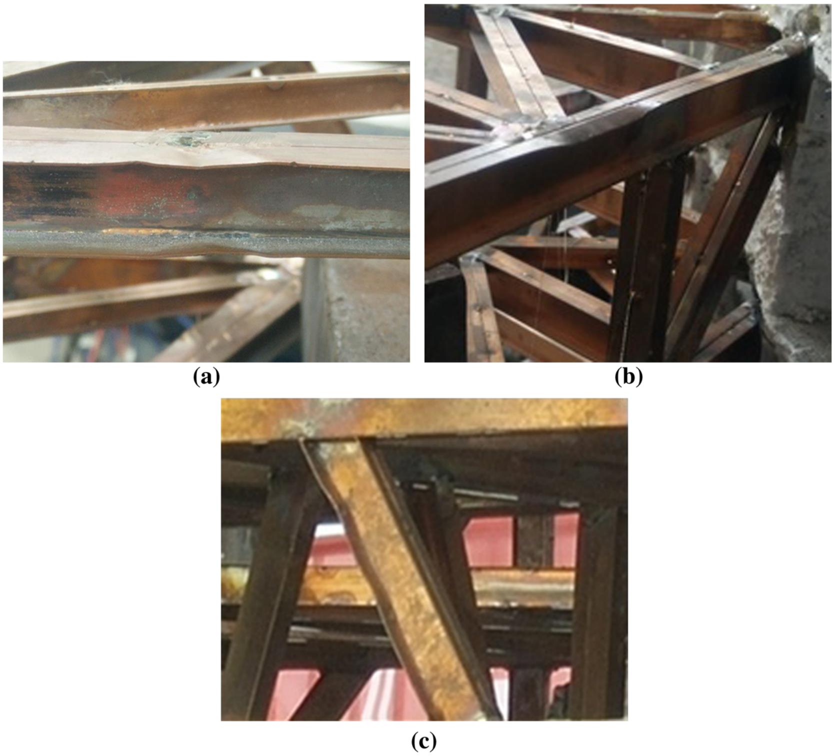

FIGURE 10 Damage of the connecting steel truss. (a) Local buckling at eighth floor. (b) Local buckling at eighth floor. (c) Local buckling at 35th floor

TABLE 6 Natural frequencies of the test model

Modal order	Initial state f (Hz)	After SLE test (PGA = 0.105 g)		After DBE test (PGA = 0.3 g)		After MCE test (PGA = 0.66 g)		After test with PGA = 0.875 g		Vibration modes
		f (Hz)	Degradation ratio	f (Hz)	Degradation ratio	f (Hz)	Degradation ratio	f (Hz)	Degradation ratio	
1st	1.95	1.90	2.6%	1.84	5.6%	1.78	8.7%	1.71	12.3%	Y-directional translation
2nd	2.09	2.06	1.4%	2.05	1.9%	1.95	6.7%	1.90	9.1%	X-directional translation
3rd	2.57	2.54	1.2%	2.44	5.1%	2.26	12.1%	2.19	14.8%	Torsion

Abbreviations: SLE, service level earthquake; DBE, design-based earthquake; MCE, maximum considered earthquake; PGA, peak ground acceleration.

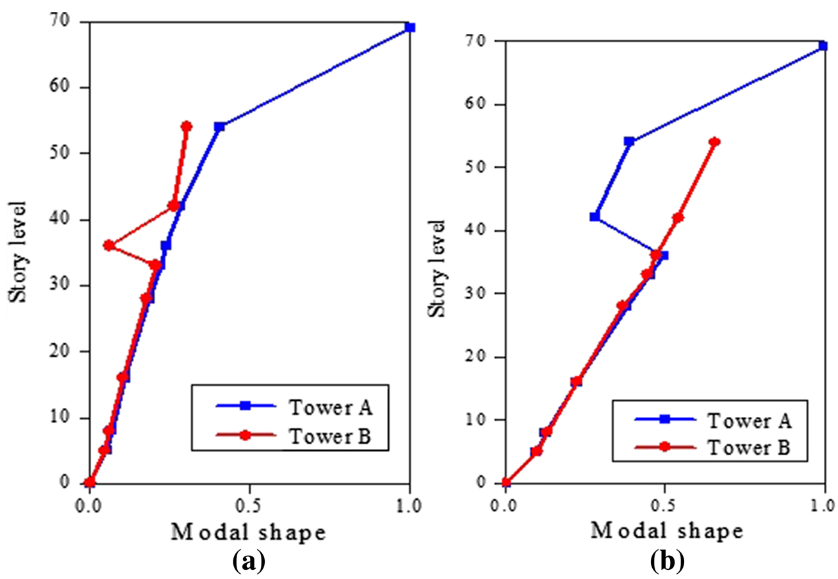

FIGURE 11 First and second vibration mode of the test model. (a) Y-directional translation. (b) X-directional translation

eighth floor where the two towers are rigidly connected by steel truss, and they are all around the beam-slab-column joint. It indicates that the connecting floors and the beam-slab-column joints are more vulnerable to seismic excitation. After MCE level loading, damage of the connecting joints has not occurred. Even at the end of the test, only slight local buckling is found in truss connection and no damage occurred in rigid connection joints between the towers and steel trusses. It illustrates that rigid connection joints performed well during the loading process. In summary, the whole structural damage is slight, and most of the lateral resistance components remain elastic. Hence, it is speculated that the test structure behaves well under strong ground motions.

4.2 | Dynamic characteristics

Dynamic characteristics of the test specimen can be obtained from the white noise tests. The first three natural frequencies are recognized and shown in Table 6. The natural frequencies decrease gradually after each loading level, and the degradation of frequencies indicate the structural

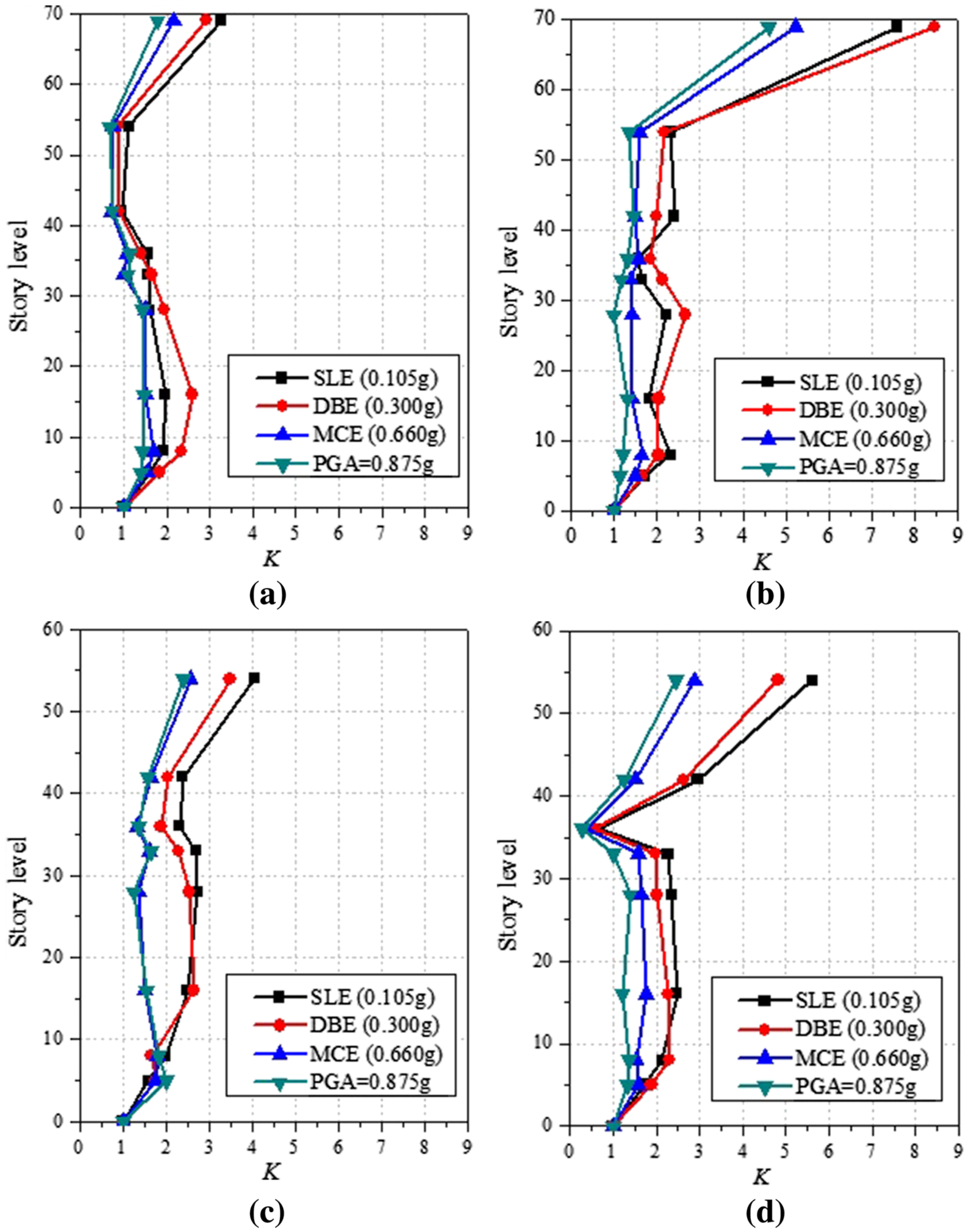

FIGURE 12 Envelope diagram of horizontal acceleration amplification Factor K. (a) X-direction of Tower A. (b) Y-direction of Tower A. (c) X-direction of Tower B. (d) Y-direction of Tower B. SLE, service level earthquake; DBE, design-based earthquake; MCE, maximum considered earthquake; PGA, peak ground acceleration

damage in a system level. There is almost no degradation for natural frequencies after SLE test, and no visible damage was observed during the test, which reveals that the test model was still in an elastic state. After DBE level loading, degradation of the first natural frequency is larger than 5%, and few corner column damages were observed, indicating that few structure members behave in a nonlinear state. The decrease of the first two natural frequencies is less than 10% after MCE level input. Even at the end of the test, decrease of the first two natural frequencies is only 12.3% and 9.1%, respectively. It illustrated that there is no serious degradation of structural lateral stiffness after the test, and the structure exhibited a good seismic performance. In addition, the first and second-order vibration modes are presented in Figure 11. It can be observed that vibration modes under 36th floor of the two towers are similar, demonstrating the significant constraint effect of the connecting truss on the vibration of the towers.

According to the Chinese code JGJ3-2011,[23] the ratio of the first-order torsional period to the first translation period is required to be less than 0.85 to prevent the excessive torsional effect in the overall structural vibration. For the test in this paper, this ratio can be calculated as 0.76. Thus, the related provision specified in the code is met.

TABLE 7 Maximum value of the vertical acceleration (g)

	SLE level			DBE level		
Floor	Tower A	Tower B	Connecting truss	Tower A	Tower B	Connecting truss
5	0.169	0.226	1.857 (at 36th floor)	0.456	0.524	7.279 (at 36th floor)
33	0.549	0.476		1.531	1.136	
55	0.792	0.560		2.609	1.509	
69	0.826			2.710		

Abbreviations: SLE, service level earthquake; DBE, design-based earthquake.

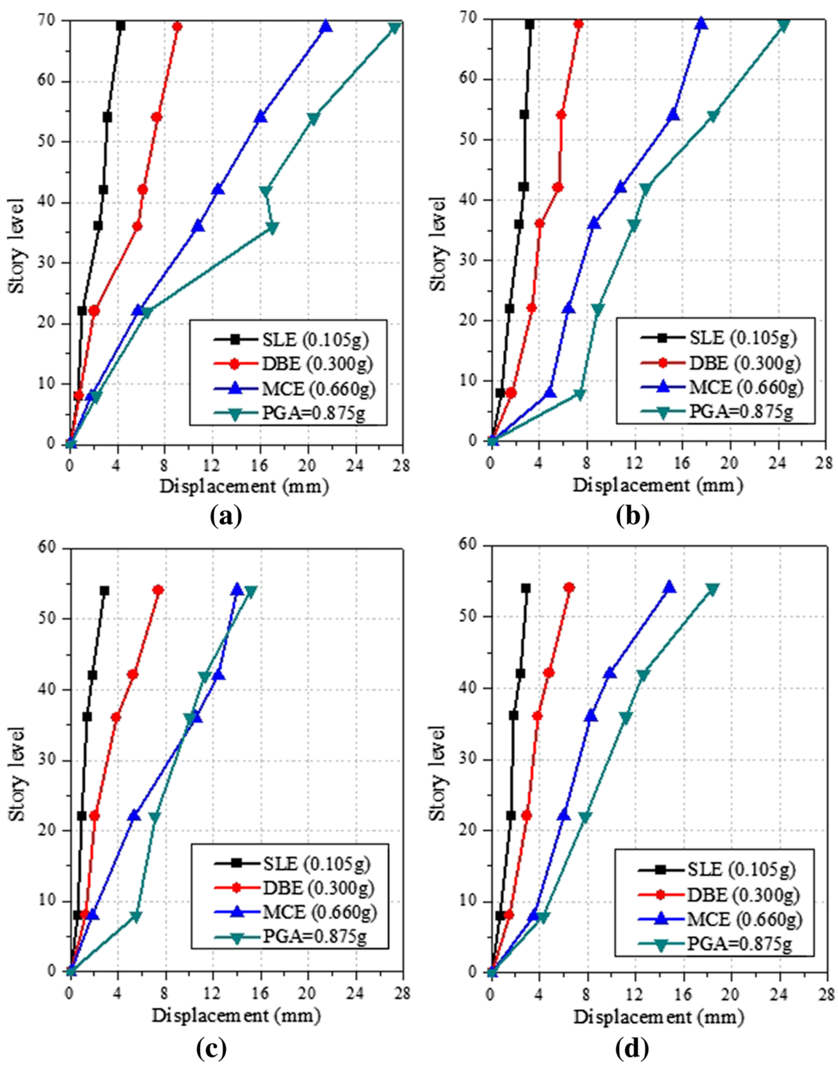

FIGURE 13 Envelope diagram of horizontal displacement responses. (a) X-direction of Tower A. (b) Y-direction of Tower A. (c) X-direction of Tower B. (d) Y-direction of Tower B. SLE, service level earthquake; DBE, design-based earthquake; MCE, maximum considered earthquake; PGA, peak ground acceleration

4.3 | Acceleration responses

The acceleration amplification factors of the two towers under each seismic level excitation are shown in Figure 12. Here, the acceleration amplification factor, *K*, is defined as the ratio of peak acceleration response to the corresponding input PGA. The structural responses are obviously affected by high-mode shape according to the response changing with the structure height. In general, the acceleration amplification factors decease gradually with the increase of input seismic intensity. It indicates that the stiffness of test structure degraded progressively. At the upper connecting floors (33rd–36th floor), the acceleration amplification factors become smaller due to the stiffness enhancement caused by the connecting trusses. Most of the acceleration amplification factors are at the range of 1–3, and all the acceleration amplification factors are less than 3 except for the roof. Acceleration amplification factors at the roof suddenly increase, especially in Y-direction, which reflects the remarkable whiplash effect of the structure and implies that restriction effect of connecting trusses on X-direction of the connected towers is larger than Y-direction.

The maximum values of vertical acceleration under SLE and DBE input are listed in Table 7. The vertical acceleration responses increase with the structure height and response of Tower A is larger than Tower B. It should note that the maximum vertical acceleration of the connecting trusses under SLE and DBE excitations is 1.857 and 7.279 g, respectively. Both are much larger than the towers' responses, illustrating the connecting trusses is very sensitive to the vertical excitations.

4.4 | Displacement responses

Envelope values of displacement responses at each floor are plotted in Figure 13. The displacement under seismic level excitations of MCE and PGA = 0.875 g is much larger than that of SLE and DBE level. And it increases faster with the structural height than SLE and DBE level. These

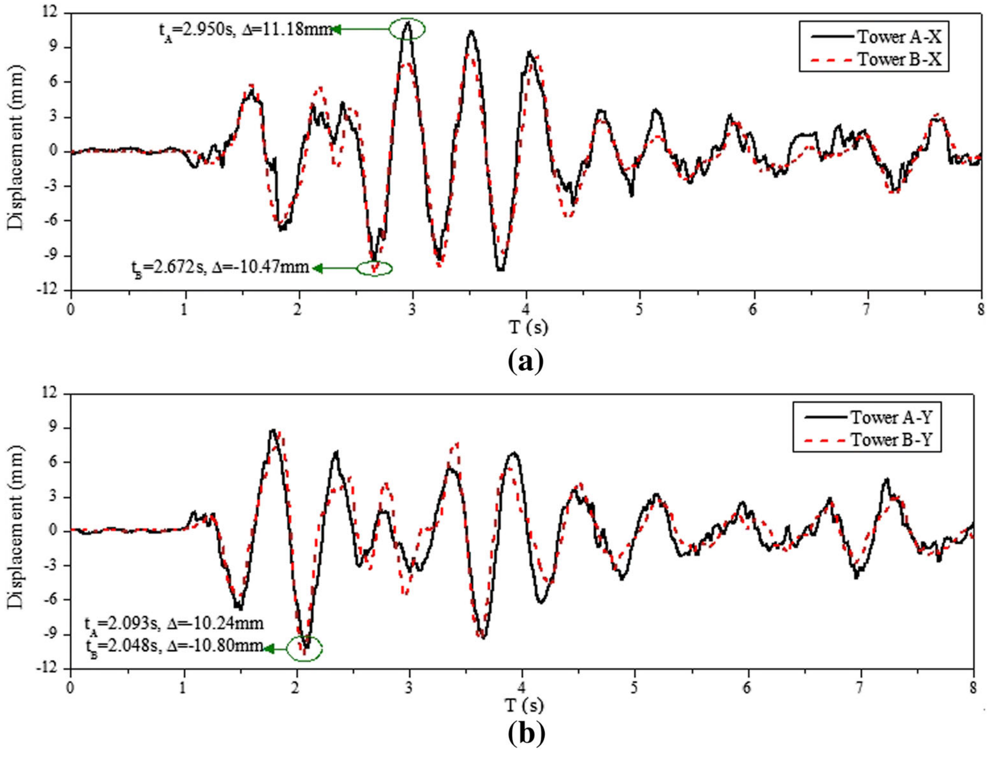

FIGURE 14 Displacement time histories of 36th floor under loading Case 27. (a) X-directional responses. (b) Y-directional responses

TABLE 8 Maximum interstory drift ratio of the test model

	SLE level		DBE level		MCE level		Level with PGA = 0.875 g	
Tower	X	Y	X	Y	X	Y	X	Y
A	1/956	1/882	1/384	1/392	1/120	1/164	1/126	1/142
B	1/1092	1/1017	1/372	1/529	1/272	1/223	1/145	1/183

Abbreviations: SLE, service level earthquake; DBE, design-based earthquake; MCE, maximum considered earthquake; PGA, peak ground acceleration.

reveal that the whole lateral stiffness of the connected structure decreases obviously under MCE excitation, which is in accordance with the degradation of natural frequencies. The degradation of first three natural frequencies has increased respectively to 8.7%, 6.7%, and 12.1% after MCE level loading. The displacement response under SLE level is proportional to the structural height on the whole, indicating that the structure remains in an elastic state. In general, the displacement curves are relatively smooth without obvious inflection, which demonstrates that the distribution of lateral stiffness along the height of the structure is reasonable. The displacement curves are more similar to a bending type rather than a shear type, which implies that deformation of RC core tube does more contribution to the structural displacement.

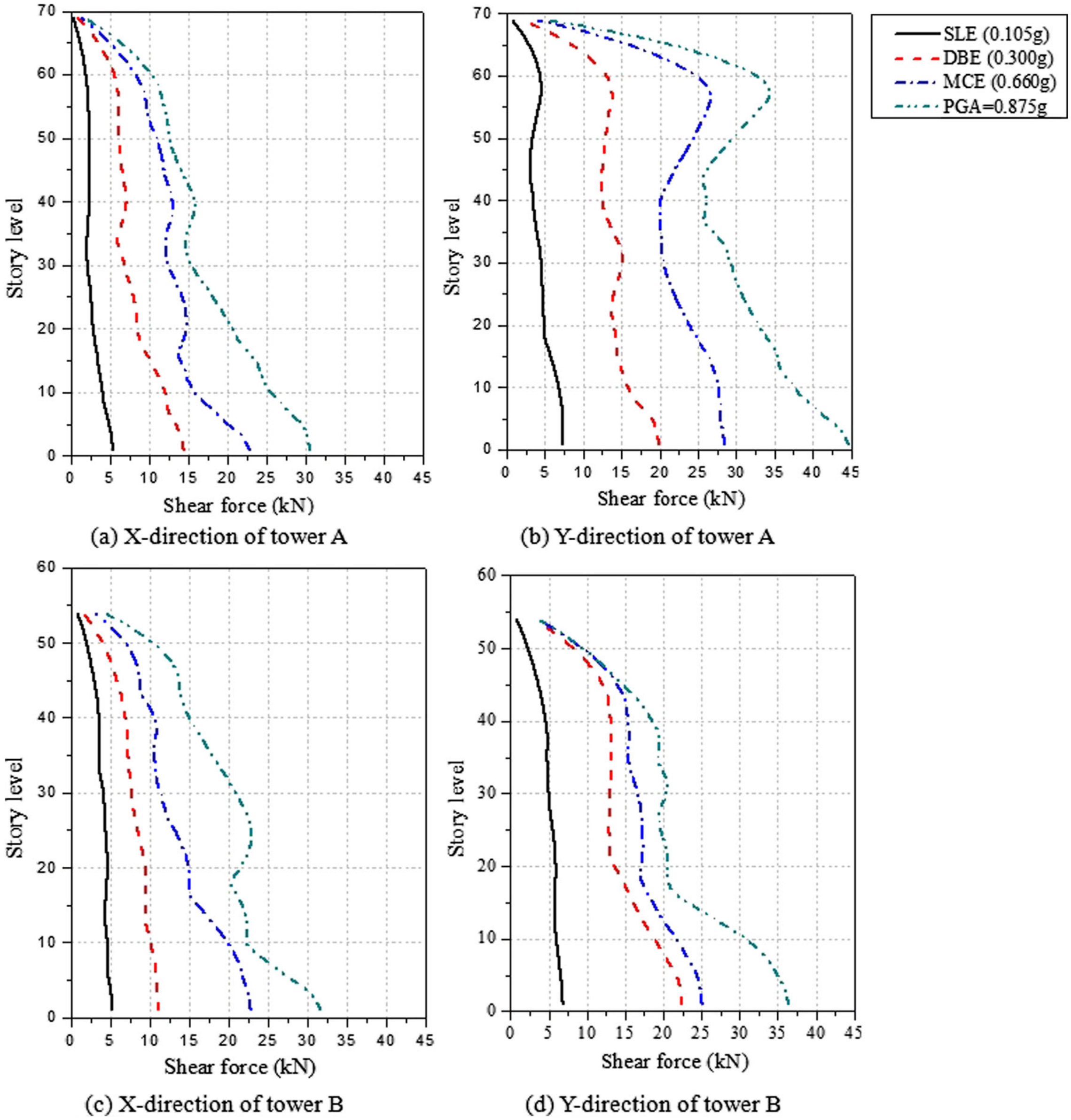

FIGURE 15 Envelope diagram of the interstory shear force of the test model. (a) X-direction of Tower A. (b) Y-direction of Tower A. (c) X-direction of Tower B. (d) Y-direction of Tower B. SLE, service level earthquake; DBE, design-based earthquake; MCE, maximum considered earthquake; PGA, peak ground acceleration

TABLE 9 Base shear coefficient of each tower of prototype structure (%)

	SLE level		DBE level		MCE level		Level with PGA = 0.875 g	
Tower	X	Y	X	Y	X	Y	X	Y
A	1.7	2.3	4.5	6.1	7.1	8.8	9.5	13.9
B	2.2	2.9	4.6	9.4	9.5	10.5	13.2	15.2

Abbreviations: SLE, service level earthquake; DBE, design-based earthquake; MCE, maximum considered earthquake; PGA, peak ground acceleration.

Figure 14 shows the X and Y-directional displacement time histories of 36th floor under bidirectional loading of seismic motion E1 with MCE level (loading Case 27). The maximum displacement value and the corresponding moment are also given. It can be observed that the displacement curves of Tower A and Tower B are basically synchronous changing with the time, which reveals that performance of the connecting trusses is able to coordinate the translational vibration of the towers.

Table 8 presents the maximum interstory drift ratios of the test model under different seismic intensity level. The peak interstory drift ratios of the connected structure during SLE level loading are 1/956 in X-direction and 1/882 in Y-direction, both of which are smaller than the elastic interstory drift limitation 1/800 in Chinese code GB50011-2010.[19] Under MCE level excitations, the peak interstory drift ratios increase to

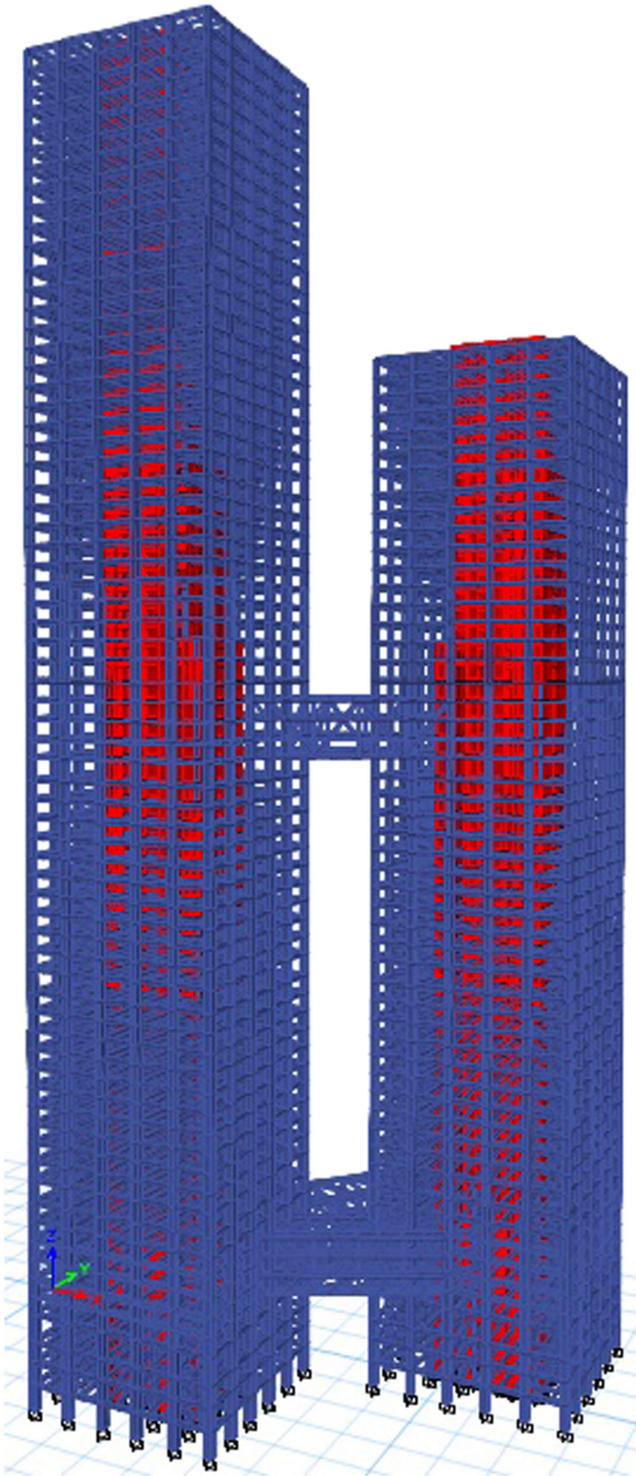

FIGURE 16 Finite element model of prototype structure

1/120 in X-direction and 1/164 in Y-direction, which are both smaller than the elastoplastic interstory drift limitation 1/100 in GB50011-2010.[19] Even under loading cases with PGA = 0.875 g, peak interstory drift ratios are still smaller than the limitation of 1/100.

4.5 | Shear force responses

The interstory shear force that reflects the magnitude of the structure internal force subjected to seismic excitation can be obtained through the measured accelerations and mass distribution of the towers. Figure 15 plots the interstory shear force distribution of the test model. The shear

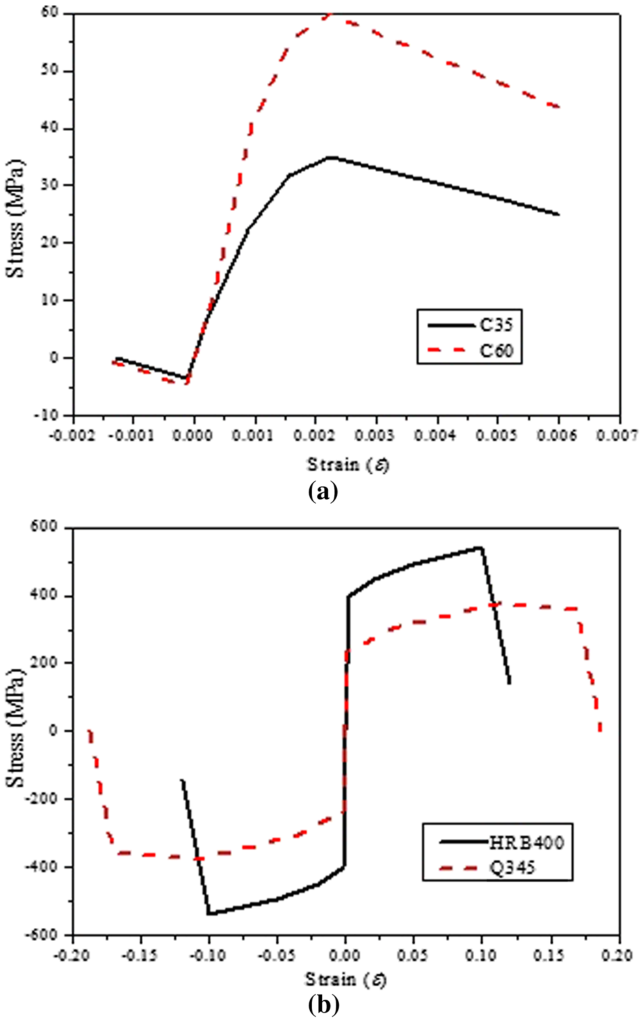

FIGURE 17 The material stress–strain relationship. (a) Concrete and (b) reinforcement and steel

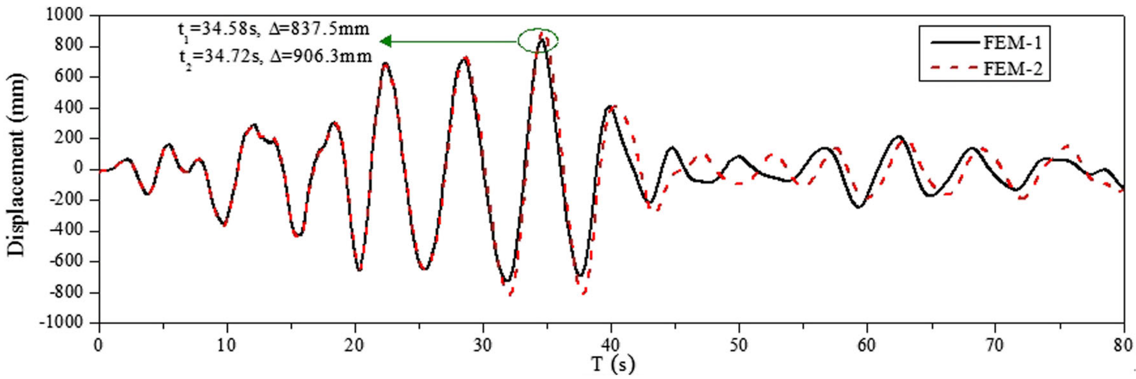

FIGURE 18 Comparison of displacement time history at the roof (69th floor). FEM, finite element model

TABLE 10 Comparison of maximum displacement responses (mm)

	Tower A			Tower B		
Floor	FEM-1	FEM-2	FEM-1/FEM-2	FEM-1	FEM-2	FEM-1/FEM-2
69	837.5	906.3	0.92			
54	613.7	640.7	0.96	476.7	504.7	0.94
42	466.2	471.4	0.99	377.4	379.8	0.99
36	379.2	383.8	0.99	318.1	319.0	1.00
22	198.0	204.5	0.97	168.5	165.5	1.02
8	42.0	42.0	1.00	36.4	35.9	1.01

Abbreviation: FEM, finite element model.

TABLE 11 Comparison of natural periods of prototype structure

Modal order	Test (T)	ETABS (E)	(E-T)/T	Vibration modes
1	5.95	6.33	6.4%	Translation in Y-direction
2	5.55	5.59	0.7%	Translation in X-direction
3	4.51	4.64	2.9%	Torsion

TABLE 12 Comparison of maximum displacement under excitation of E1 scaled to MCE level (mm)

	X-directional loading (E1-X)						Y-directional loading (E1-Y)					
	Tower A			Tower B			Tower A			Tower B		
Floor	Test	ETABS	E/T	Test	ETABS	E/T	Test	ETABS	E/T	Test	ETABS	E/T
69	799.8	837.5	1.05				890.1	1,099.0	1.23			
54	621.2	613.7	0.99	543.7	476.7	0.88	770.2	835.1	1.08	505.1	569.6	1.13
42	471.6	466.2	0.99	417.2	377.4	0.91	518.2	590.0	1.14	365.7	436.6	1.19
36	345.0	379.2	1.10	389.6	318.1	0.82	408.0	472.7	1.15	321.4	365.9	1.14
22	215.4	198.0	0.92	173.7	168.5	0.97	254.5	229.1	0.90	203.8	191.9	0.94
8	71.9	42.0	0.58	66.8	36.4	0.54	63.8	45.9	0.72	60.8	40.7	0.67

Abbreviation: MCE, maximum considered earthquake.

TABLE 13 Comparison of maximum acceleration under excitation of E1 scaled to MCE level (g)

	X-directional loading (E1-X)						Y-directional loading (E1-Y)					
	Tower A			Tower B			Tower A			Tower B		
Floor	Test	ETABS	E/T	Test	ETABS	E/T	Test	ETABS	E/T	Test	ETABS	E/T
69	0.45	0.43	0.96				0.96	0.39	0.41			
54	0.11	0.24	2.18	0.41	0.32	0.78	0.26	0.28	1.08	0.51	0.35	0.69
42	0.11	0.25	2.27	0.25	0.27	1.08	0.25	0.25	1.00	0.31	0.27	0.87
36	0.19	0.30	1.58	0.22	0.30	1.36	0.18	0.24	1.33	0.08	0.26	3.25
33	0.17	0.29	1.71	0.24	0.30	1.25	0.17	0.22	1.29	0.25	0.27	1.08
28	0.18	0.22	1.22	0.24	0.25	1.04	0.21	0.23	1.10	0.25	0.26	1.04
16	0.26	0.27	1.03	0.28	0.30	1.07	0.27	0.26	0.96	0.26	0.27	1.04
8	0.26	0.29	1.12	0.28	0.30	1.07	0.24	0.21	0.875	0.29	0.34	1.17
5	0.27	0.27	1	0.29	0.27	0.93	0.3	0.3	1.00	0.29	0.31	1.07

Abbreviation: MCE, maximum considered earthquake.

forces increase with the shaking intensity. But the growth rate slows down during loading level of MCE and PGA = 0.875 g in terms of the increase of input PGAs, which is induced by the degradation of structural stiffness after MCE level loading. According to the similarity theory, base shear coefficient, defining as the ratio of base shear to structural weight, of the prototype structure can be calculated, as listed in Table 9. Under SLE level excitation, the base shear coefficient in X-direction is 1.7% and 2.2% for each tower and in Y-direction is 1.7% and 2.2%, respectively. Both of them are larger than the minimum value 1.2% specified in GB50011-2010[23] and JGJ3-2011.[24] These base shear coefficients increase progressively with the increasing seismic intensity and are within reasonable ranges.[1,10]

5 | NUMERICAL ANALYSIS OF PROTOTYPE STRUCTURE

5.1 | Finite element model

The software program ETABS is employed to establish the finite element model (FEM) of prototype structure for further seismic performance investigation. The beams and columns are simulated by frame element, as well as braces and truss members. To consider the nonlinear behavior of frame element, plastic hinges should be assigned for the key members. According to the shaking table test, damages are concentrated on the connecting floors and trusses. Therefore, plastic hinges are only assigned for frame elements at first to eighth and 33rd–36th floor. The floor slabs which are assumed to be elastic are modeled by membrane element. Because the shear walls at the bottom floors are more like to be damaged, the

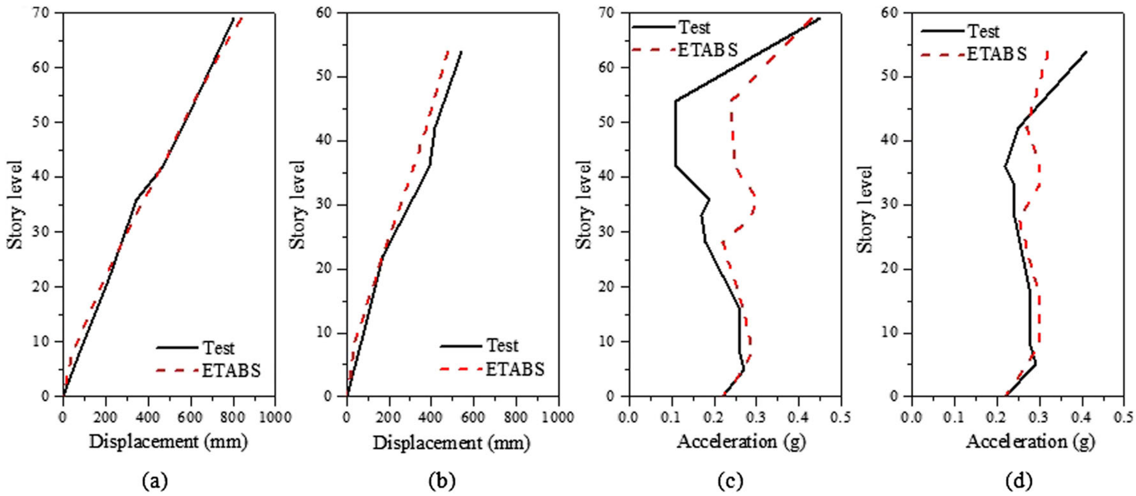

FIGURE 19 Result comparison under E1-X excitation scaled to maximum considered earthquake level. (a) Displacement of Tower A. (b) Displacement of Tower B. (c) Acceleration of Tower A. (d) Acceleration of Tower B

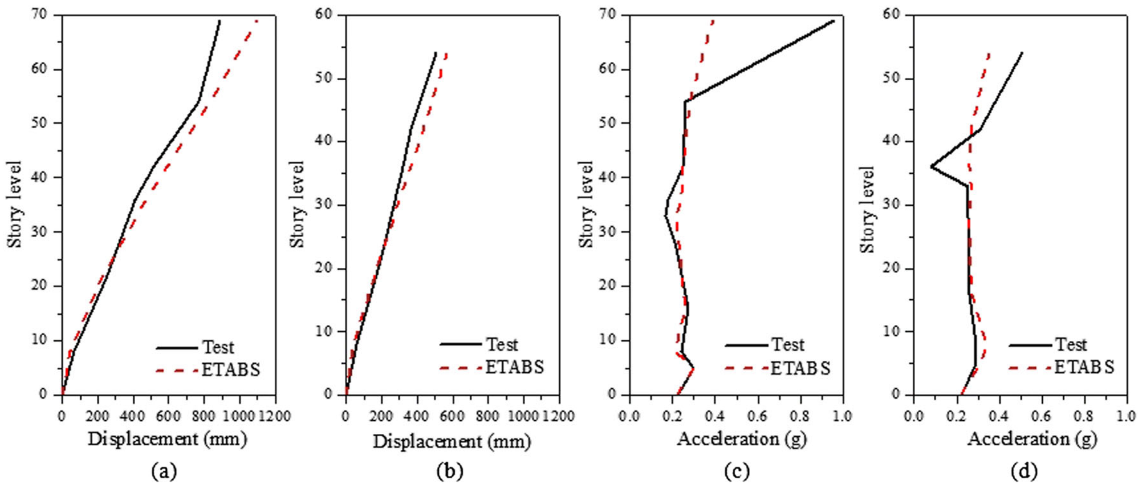

FIGURE 20 Result comparison under E1-Y excitation scaled to maximum considered earthquake level. (a) Displacement of Tower A. (b) Displacement of Tower B. (c) Acceleration of Tower A. (d) Acceleration of Tower B

walls at first to fifth floor are modeled by multilayer shell element to consider the wall's nonlinear behavior. The shell-thin element is adopted for other shear walls. Hinged joints in this model are achieved by releasing the corresponding end moment. The Rayleigh damping is utilized for this model, and damping ratio is adopted as 0.05. The sum of nodes and elements are 140624 and 289066, respectively, including177621 frame elements and 111445 shell elements. And the number of plastic hinge is 2,206. Figure 16 shows the three-dimensional analysis model of prototype structure. And the stress–strain relationships of materials, which adopt the model in ETABS, are plotted in Figure 17. Meanwhile, confined concrete is considered for steel tube-RC column by using the Mander's model in ETABS.

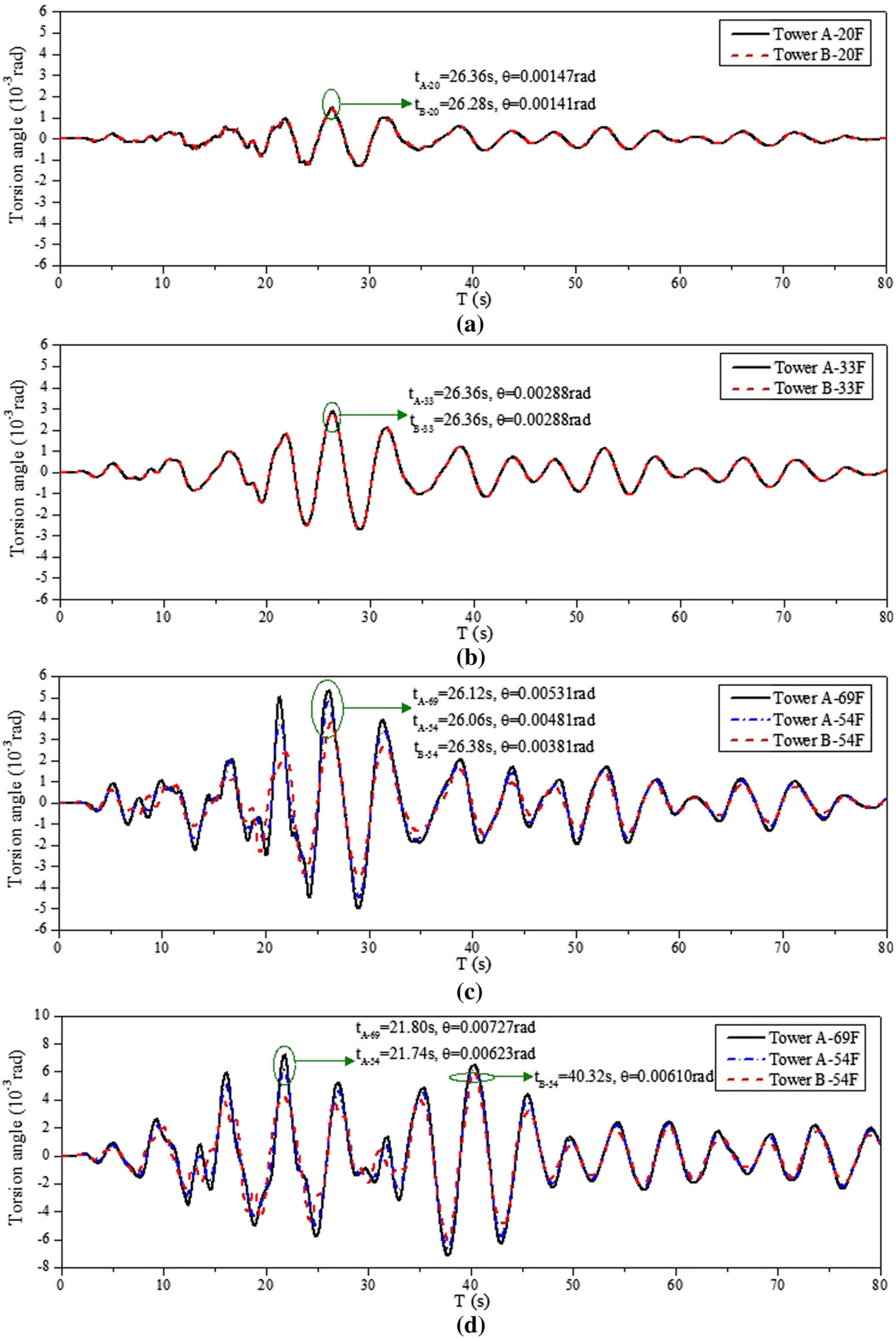

FIGURE 21 Torsion responses of connected structure under E1-X and E1-Y excitation scaled to maximum considered earthquake level. (a) Responses at 20th floor under E1-X excitation. (b) Responses at 33rd floor under E1-X excitation. (c) Responses at 69th and 54th floor under E1-X excitation. (d) Responses at 69th and 54th floor under E1-Y excitation

To verify the computational accuracy of the analytical model above, the nonlinear plastic hinges are extended to 40th floor. The analytical model that plastic hinges is assigned for frame elements at first to eighth and 33rd–36th floor is marked as FEM-2 (FEM-1) here. The model with plastic hinges at first to 40th floor is defined as FEM-2. Nonlinear time history analyses under X-directional loading of ground motion E1 scaled to MCE level are conducted for the two analytical models. Figure 18 compares the displacement time history and Table 10 lists the comparison of

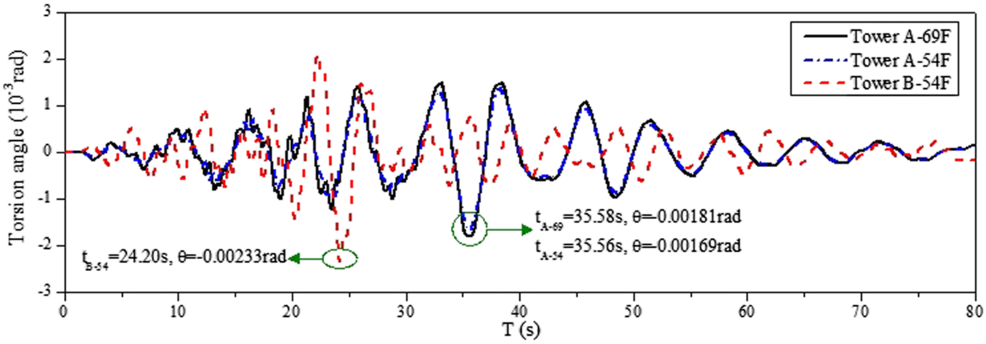

FIGURE 22 Torsion responses of single tower without connecting trusses under E1-X excitation scaled to maximum considered earthquake level

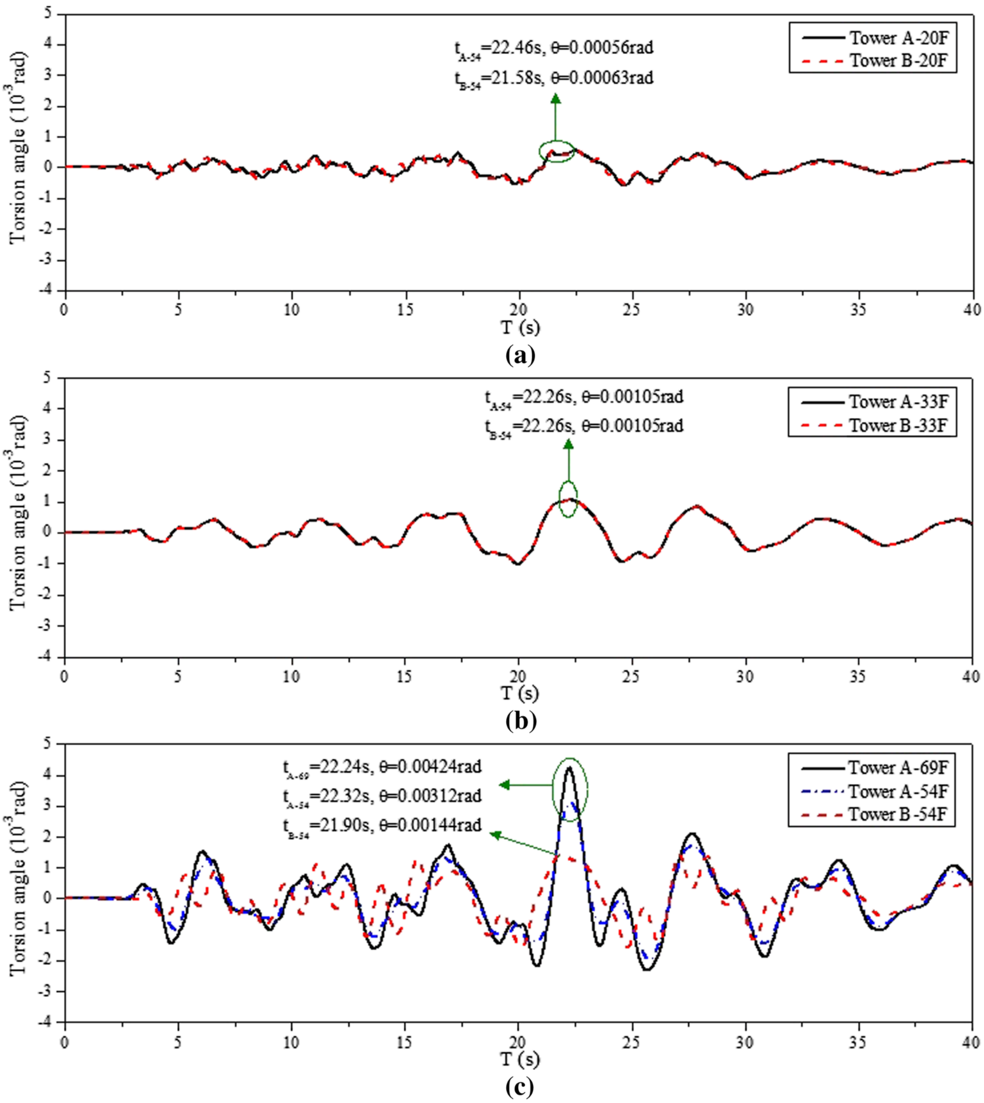

FIGURE 23 Torsion responses under three-directional excitation of artificial motion scaled to maximum considered earthquake level. (a) Responses at 20th floor. (b) Responses at 33rd floor. (c) Responses at 69th and 54th floor

maximum displacement responses. It can be observed that response of FEM-1 has a good match with FEM-2. Although the plastic hinges of FEM-1 are only assigned at first to eighth and 33rd–36th floor, it still has high computational accuracy. Meanwhile, the FEM-1 has a great advantage over FEM-2 in terms of saving computation time. Therefore, the FEM-1 model is adopted for the following analyses.

5.2 | Comparison of experimental and numerical results

Based on the similarity scaling factors shown in Table 4, natural periods of the test model can be extrapolated to the periods of prototype structure. The first three natural periods of prototype structure extrapolated from the shaking table test are 5.95, 5.55, and 4.51 s, respectively. The comparison for periods of the test and ETABS is given in Table 11. It can be found that the numerical results show a good agreement with the experimental results. The distribution of mass and stiffness between the test model and prototype structure meets the relationship of similar design.

Nonlinear time history analyses under X-directional and Y-directional loading of ground motion E1 scaled to MCE level, corresponding to loading Cases 25 and 26 shown in Table 5, are conducted for the prototype structure. Note that PGA of MCE level excitation for the prototype is 0.22 g. Tables 12 and 13 compare the maximum displacement and acceleration responses of the test and numerical analyses. Among them, the test result for prototype is extrapolated from experimental data. To better display the result comparison, Figures 19 and 20 plot the results under X-directional loading and Y-directional loading, respectively. The displacement responses of each tower agree well with the test result in general. Under X-directional loading, the discrepancy between test and numerical analyses for most floors is less than 10%. Under Y-directional loading, the discrepancy becomes a little larger, but most of them are less than 15%. Although the discrepancy for acceleration responses is relatively large, test and numerical results at many floors are approximate, and the trend changing with structural height is similar on the whole. In general, the numerical results are in accordance with the test. The main reasons for the discrepancies include (a) model materials cannot accurately simulate the prototype material; (b) errors exist in the construction process; (c) size effect is inevitable in such scaled model test. Moreover, considering the connecting trusses in the test specimen are simulated by copper plate, the impact of above factors on dynamic performance of connecting trusses is slight.

5.3 | Performance of connecting trusses

Because the connecting trusses are designed to coordinate the deformation of the two towers, the performance of the trusses is critical during vibration of the towers. It should be equipped with adequate stiffness to coordinate the two towers to resist lateral forces together. Although the two single towers without truss connection differ greatly in fundamental period (for Tower A is 6.740 s and for Tower B is 5.037 s), the connecting trusses are still capable of coordinating the towers' translational displacement, which is demonstrated by the test in Section 4.4. Considering torsion effect has a great influence on the performance of connecting trusses, capacity of connecting trusses to coordinate torsional deformation is evaluated here based on the numerical results.

Figure 21 shows the torsion angle time histories under excitation of seismic motion E1 scaled to MCE level. The maximum value of torsion angle at each floor and the corresponding moment are also given. Moreover, torsion responses of single tower without connecting trusses under E1-X excitation are plotted in Figure 22. By comparison, it can be found that torsional deformation of the connected structure is much larger than single tower without connecting trusses. The remarkable torsional deformation will present a great challenge to the performance of diagonal connecting trusses. From Figure 21, two torsion angle curves are complete overlap in general at 22th floor and 33rd floor. At the roof (69th floor for Tower A and 54th floor for Tower B), torsional deformation of Tower A is obviously larger than that of Tower B, but they vibrate in phase on the whole. These imply that torsional deformation of the two towers coincides with each other.

As the long-span truss is very sensitive to vertical excitations, three-directional excitation of artificial motion scaled to MCE level is input to the numerical model. The corresponding torsional responses are shown in Figure 23. It can be observed that two torsion angle curves are complete overlap basically at 33rd floor where the high zone connecting trusses locate at. Although the torsional responses of the towers are not

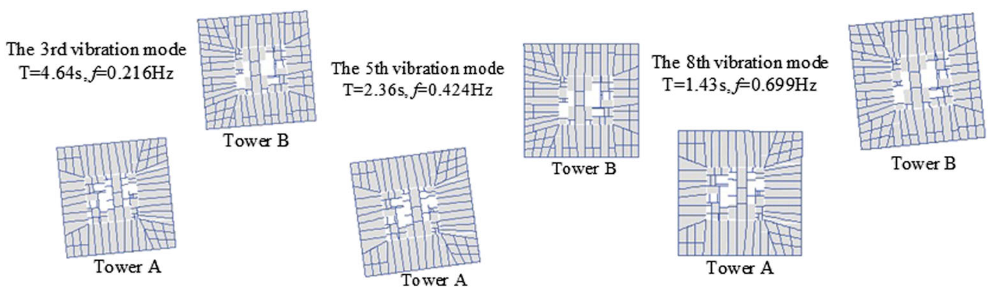

FIGURE 24 Overall torsional mode and single tower torsional mode of the connected structure

synchronous changing with the time at 20th floor and the roof, the overall changing trend of the curves are consistent. It also can be found that torsional responses at 20th floor and the roof of Tower B vibrate with larger frequency than Tower A, which is resulted from the high-order torsional mode. Figure 24 shows the overall torsional mode and single tower torsional mode of the connected structure. The frequency of torsional mode of single Tower B is 0.699 Hz, which is 1.65 times that of single Tower A. This explains why torsional responses of the towers are not completely synchronous at 20th floor and the roof. In summary, the performance of connecting trusses is able to coordinate torsional deformation of the two towers and make them resist lateral forces together even under MCE level excitations. Although the high torsional modes are triggered, the performance of connecting trusses to coordinate deformation is still reliable.

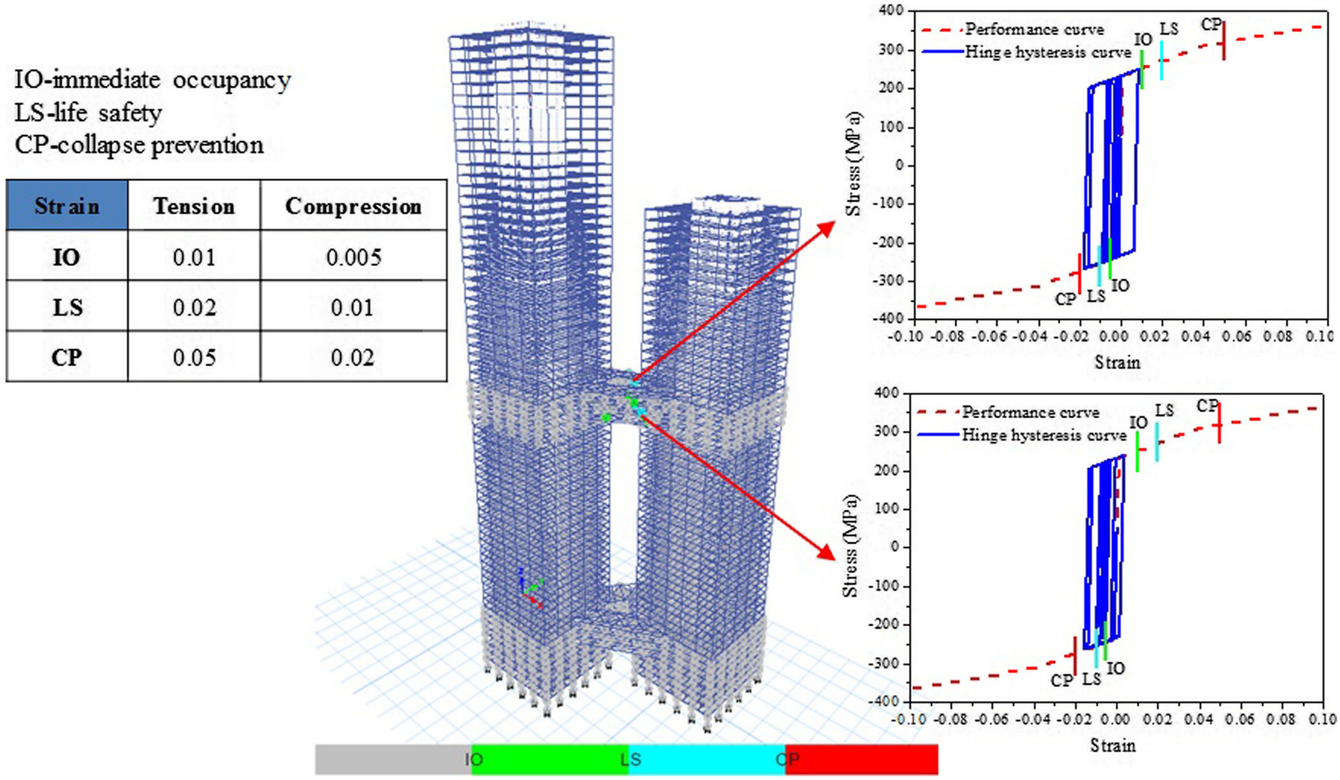

FIGURE 25 State of plastic hinges under three-directional excitation of artificial motion scaled to maximum considered earthquake level

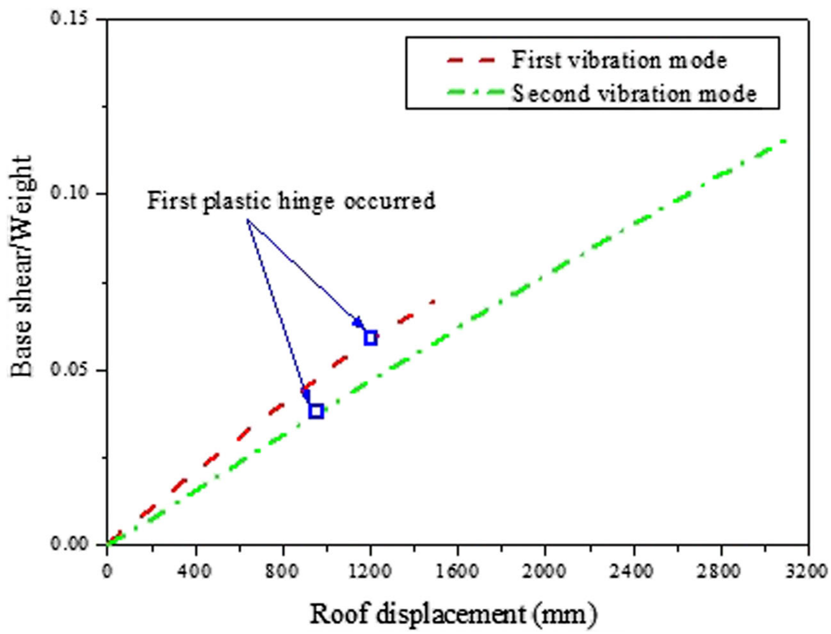

FIGURE 26 Pushover curves of the structure

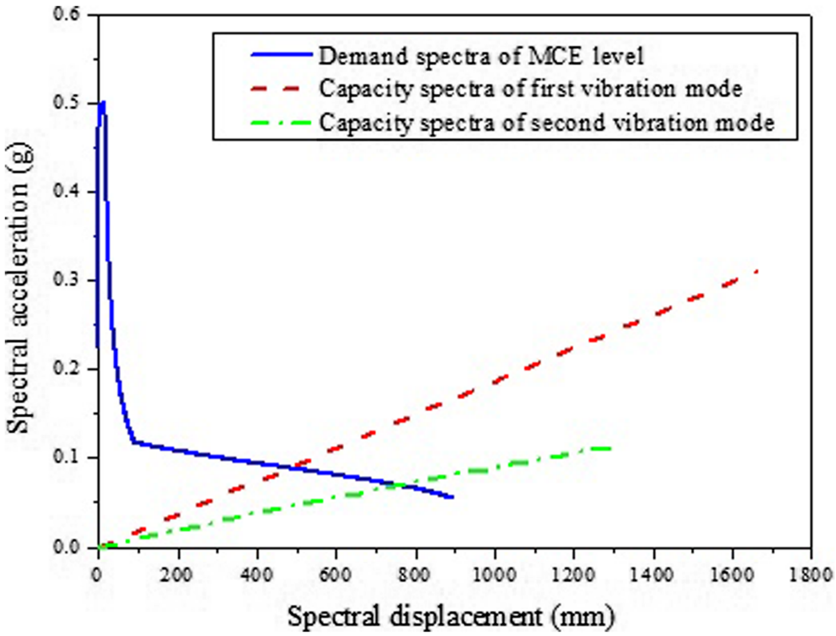

FIGURE 27 Capacity and demand spectra. MCE, maximum considered earthquake

Moreover, the state of plastic hinges under three-directional excitation of artificial motion scaled to MCE level is plotted in Figure 25, and two hinge hysteresis curves in structure members that are damaged most seriously are also presented. The acceptance criteria strains shown in Figure 25 are suggested by ASCE 41-13.[27] From this figure, the overall damage of the structure is slight. In the connecting trusses, only few truss web members are damaged and most serious damage does not attain to collapse prevention state. Therefore, it can deem that the performance of connecting trusses is able to resist strong ground motions while coordinating the two towers' deformation.

In order to evaluate the ultimate capacity of the prototype furtherly, the modal pushover analysis,[28] considering the response due to the first two modes, is implemented for the connected structure. Figure 26 shows the X-directional pushover curves of the structure, and the corresponding capacity spectra are plotted in Figure 27. The demand spectrum is obtained by the Chinese code.[23] It can be observed that the structure has strong deformability, and the capacity is much larger than the demand. It can be deemed that the structure has a high ultimate capacity to resist strong seismic motions.

6 | CONCLUSIONS

In this paper, a 1/45 scaled model of an asymmetrical twin-tower super high-rise building rigidly connected by long-span steel truss is constructed and subsequently tested on the shaking table to investigate the seismic performance. The structural damage evolution, dynamic characteristics, and responses are analyzed based on the test results. Moreover, a three-dimensional FEM for the prototype structure is built and time history analyses are performed. The following conclusions can be obtained:

1. The structural damage firstly appeared under DBE level excitations. The damage pattern includes fine crack and local concrete spalling of frame corner columns, as well as local buckling of connecting trusses. All the damages concentrate on the connecting floors, which are more vulnerable to seismic excitation and are the weak floors. At the end of the test, no damage occurred in rigid connection joints between the towers and connecting trusses. The whole structural damage is slight and most of the lateral resistance components remain elastic.
2. There is almost no degradation of natural frequencies after SLE level loading and no visible damage was observed, and the test model was still in an elastic state. After MCE level loading, whole lateral stiffness of the connected structure decreases. But degradation of the first two natural frequencies is less than 10%. The structural lateral stiffness is still sufficient to resist seismic excitations. Meanwhile, the connecting trusses behave with no visible damage during MCE level loading.
3. The lateral deformation mode of the structure is dominated by bending deformation. The peak interstory drift ratios during SLE level excitations are 1/956 in X-direction and 1/882 in Y-direction, both of which are smaller than the elastic interstory drift limitation 1/800 in Chinese code.[19] The peak interstory drift ratios under MCE level excitations are 1/120 in X-direction and 1/164 in Y-direction, which are both smaller than the elastoplastic interstory drift limitation 1/100.[19] Moreover, it should note that the whiplash effect at the roof of the structure is serious and the connecting trusses are very sensitive to the vertical excitations.

4. The result of numerical analysis shows a good agreement with the test results on the whole. It demonstrates that scaled model test is an effective method to investigate the whole structural failure mechanism and seismic performance of complex super high-rise building, although it has some limitations, such as size effect and construction error.
5. According to the numerical results, the performance of connecting trusses is able to coordinate translational and torsional deformation of the two towers and make them resist lateral forces together. Although the high torsional modes are triggered, the performance of connecting trusses to coordinate deformation is still reliable.
6. The seismic performance of the structure is commendable. The connecting trusses and rigid connection joints behave well during strong seismic excitations, indicating the design of the connected structure is reliable and reasonable. The research in the paper is expected to be an important reference for the design of complex connected structures.

ACKNOWLEDGMENTS

The authors are grateful for the financial support from the Fundamental Research Funds for the Central Universities of Central South University (Project 502221804), the National Natural Science Foundation of China (Project 51878674), the Foundation for Key Youth Scholars in Hunan Province (Project 150220077), and the Project of Yuying Plan in Central South University (Project 502034002). Any opinions, findings, and conclusions or recommendations expressed in this paper are those of the authors.

ORCID

Zhipeng Zhai https://orcid.org/0000-0002-9646-2677

REFERENCES

[1] X. Lu, Y. Zou, W. Lu, B. Zhao, *Earthquake Eng. Struct. Dyn.* **2007**, *36*, 439.
[2] H. Fan, Q. Li, A. Tuan, L. Xu, *J. Construct. Steel Res.* **2009**, *65*, 1206.
[3] Q. Chen, W. Yuan, Y. Li, L.-y. Cao, *J. Cent. S. Univ.* **2013**, *20*(5), 1341.
[4] X. Wu, J. Wang, J. Zhou, *Shock Vib.* **2018**, *2018*, 1865761. 19 pages
[5] A. Nishimura, H. Yamamoto, Y. Kimura, H. Kimura, M. Yamamoto, A. Kushibe, *Struct. Concr.* **2011**, *12*(2), 94.
[6] X. Lu, Q. Lu, W. Lu, Y. Zhou, B. Zhao, *Structural Control and Health Monitoring* **2017**, *25*(3), e2109.
[7] J. Kim, J. Ryu, L. Chung, *Eng. Struct.* **2006**, *28*(2), 183.
[8] C. C. Patel, R. S. Jangid, *Struct. Control Health Monit.* **2014**, *21*(2), 205.
[9] Y. Zhou, X. Lu, W. Lu, Z. He, *Earthquake Eng. Eng. Vib.* **2009**, *8*(1), 47.
[10] X. Lu, L. Chen, Y. Zhou, Z. Huang, *Struct. Des. Tall Spec.* **2010**, *18*(7), 765.
[11] D. Zhou, C. Guo, X. Wu, B. Zhang, *Shock Vib.* **2016**, *2016*, 8215696, 18 pages.
[12] X. Wu, Y. Sun, M. Rui, M. Yan, L. Li, D. Liu, *Comput. Concr.* **2013**, *12*(2), 211.
[13] C. Li, Research on dynamic reliability and damping control theory of high-rise connection structure (PhD Thesis), *Lanzhou University of Technology*, Lanzhou, **2018** (in Chinese).
[14] P. Abbasi Maedeh, A. Ghanbari, W. Wu, *Geomech. Eng.* **2017**, *12*(6), 949.
[15] P. A. Maedeh, A. Ghanbari, W. Wu, *Earthquake Struct.* **2017**, *12*(2), 145.
[16] H. Abdollahiparsa, P. Homami, F. Khoshnoudian, *KSCE J. Civ. Eng.* **2016**, *20*(7), 1.
[17] P. Homami, K. Kumarci, A. B. Dehkordy, Using support vector machine model to study of dynamic response of guyed tower subjected to earthquake loading, Proceedings of 8th National Congress on Civil Engineering, Babol, Iran, **2014**, 1-7.
[18] X. Lu, Y. Chen, Y. Mao, *Struct. Des. Tall Spec.* **2012**, *21*(10), 699.
[19] X. Lu, G. Fu, W. Shi, W. Lu, *Struct. Des. Tall Spec.* **2010**, *17*(1), 181.
[20] H. R. Tabatabaiefar, B. Mansoury, *Struct. Des. Tall Spec.* **2016**, *25*(8), 357.
[21] W. Guo, Z. Zhai, Y. Cui, Z. Yu, X. Wu, *Eng. Struct.* **2019**, *181*, 562.
[22] Z. Lu, X. Chen, X. Lu, Z. Yang, *Earthq. Eng. Struct. Dyn.* **2016**, *45*(9), 1537.
[23] GB 50011-2010, *CODE for Seismic Design of Buildings*, China Architecture and Industry Press, Beijing **2010** (in Chinese).
[24] JGJ3-2011, *Technical Specification for Concrete Structures of Tall Building*, China Architecture and Industry Press, Beijing **2010** in Chinese.
[25] X. Lu, B. Zhou, B. Zhao, W. Lu, *Struct. Des. Tall Spec.* **2015**, *24*(18), 1019.
[26] H. G. Harris, *Structural Modeling and Experimental Techniques*, 2nd ed., CRC Press, Boca Raton **1999**.
[27] ASCE 41-13, *Seismic Evaluation and Retrofit of Existing Buildings*, American Society of Civil Engineers, Reston, VA **2014**.
[28] A. K. Chopra, R. K. Goel, *Earthquake Eng. Struct. Dynam.* **2002**, *31*(3), 561.

AUTHOR BIOGRAPHIES

Wei Guo is an associate professor of School of Civil Engineering, Central South University. His research interests are seismic isolation design, and shaking table test technology and equipment control.

Zhipeng Zhai is a PhD candidate of School of Civil Engineering, Central South University. His research focuses on structural seismic performance evaluation and seismic resilient design.

Hanfeng Wang is a professor of School of Civil Engineering, Central South University. His research interests are structural wind engineering.

Qiongxiang Liu is the chief engineer of Shenzhen General Institute of Architectural Design and Research Co., LTD. He received his bachelor degree from Wuhan University of Technology in 1982. His interests are seismic performance of complex structure, and structural design.

Kai Xu is a R&D engineer of Design and Research Department for New Building Systems & Materials, Shenzhen General Institute of Architectural Design and Research Co., LTD. He received his doctoral degree from Guangzhou University in 2017. His interests are seismic isolation and seismic control.

Zhiwu Yu is a professor of School of Civil Engineering, Central South University. His research interests are design theory and application of steel-concrete composite structure, and dynamic calculation theory of high-speed railway bridges.

How to cite this article: Guo W, Zhai Z, Wang H, Liu Q, Xu K, Yu Z. Shaking table test and numerical analysis of an asymmetrical twin-tower super high-rise building connected with long-span steel truss. *Struct Design Tall Spec Build*. 2019;e1630. https://doi.org/10.1002/tal.1630